DYNAMIC ANALYSIS OF A TRANSMISSION LINE TERMINATED BY A BISTABLE AMPLIFIER

By

BALAKRISHNA MUDUNURI

Bachelor of Science
Andhra University
Waltair, India
1964

Bachelor of Engineering
Andhra University
Waltair, India
1967

Master of Science in Engineering
Indian Institute of Science
Bangalore, India
1971

Submitted to the Faculty of the Graduate College
of the Oklahoma State University
in partial fulfillment of the requirements
for the Degree of
MASTER OF SCIENCE
May, 1973

OKLAHOMA
STATE UNIVERSITY
LIBRARY

OCT 9 1973

DYNAMIC ANALYSIS OF A TRANSMISSION LINE TERMINATED BY A BISTABLE AMPLIFIER

Thesis Approved:

Karl N. Reid
Thesis Adviser

Jerald D. Parker

Henry R. Sebesta

D. D. Durham
Dean of the Graduate College

ACKNOWLEDGEMENTS

The author wishes to express his profound sense of gratitude and appreciation to Dr. Karl N. Reid for suggesting this problem and for providing valuable suggestions and assistance. His creative genius, great research capabilities, and critical reasoning have a profound influence on the author in many respects. The author also wishes to acknowledge the helpful suggestions of Dr. H. R. Sebesta.

Special thanks are due to his wife, Rajeswari, for her patience, understanding, and encouragement during the more trying moments.

Finally he wishes to acknowledge Mrs. Barbara Moore for her elegant typing of the thesis.

TABLE OF CONTENTS

LIST OF TABLES

LIST OF ILLUSTRATIONS

NOMENCLATURE

A, B, C, D, E, F	- Constants
a	- Cross-sectional area of the line, in.^{2}
b_c	- Control port width, in.
b_s	- Supply port width, in.
C_0	- Acoustic velocity of the fluid, in/sec
d_p	- Depth of the amplifier, in.
d_0	- Diameter of the line, in
E_1	- Control to supply jet momentum ratio
j	- $\sqrt{-1}$
J_0, J_1, J_2	- Bessel functions of the first kind
$J_c(t)$	- Control jet momentum at any time t
J_s	- Supply jet momentum
k	- r_0^2/ν_0
ℓ	- Length of the line, in.
M(s), N(s)	- Polynomials in s of order m and n respectively
n	- Order of approximation
P_a, P_b	- Upstream and downstream pressures of the line respectively, psig
P_s	- Supply pressure, psig

P_1	- $k/5.78$
P_2	- $k/56.6$
P_3	- $k/40.9$
p_{bubble}	- Bubble pressure, psig
P_{sw}	- Switching pressure, psig
r_0	- Radius of the line, in.
s	- Laplace variable, $sec.^{-1}$
T_e	- ℓ/C_0
T_1	- $T_e^2 A/k$
T_2	- $9T_1$
T_3	- $25T_1$
T_4	- $49T_1$
t	- time, sec.
$U_s(t)$	- Unit step function
W_a, W_b	- Mass flow rates corresponding to P_a, P_b respectively, $lb._m/sec.$
W_s	- Supply mass flow rate, $lb._m/sec.$
X, Y	- Coordinates
Z_0	- C_0/a
$Z_c(s)$	- Characteristic impedance of the line, $(in.-sec.)^{-1}$
Z_R	- Load impedance, $(in.-sec.)^{-1}$
$\alpha_{i,n}$	- Roots of the Bessel's equation, $J_i(\alpha_{i,n})$
γ	- Ratio of specific heats

σ	- Prandtl number
ν_0	- Kinematic viscosity of the fluid, in.^{2}/sec.
$\Gamma(s)$	- Propogation operator
$\psi(t)$	- Jet deflection angle at anytime, t

CHAPTER I

INTRODUCTION

In any application of fluid logic and control devices involving high power level, and/or fast dynamic response, line dynamics effects must be included in the analysis. For instance, neglecting line dynamics effects in a digital fluidic circuit may cause dynamic hazards. (A dynamic hazard is the occurrence of an unplanned state due to time delays.) It has long been recognized that the accuracy of analytical design of a fluidic system depends on the validity of the mathematical models for the system components.

The purpose of this thesis was to study the effect of input pulse characteristics on the switching time of a fluidic logic element (more specifically a flip flop) in correlation with the pulse form from a transmission line. For this study the theoretical model developed by Epstein [1, 2][1] for the end wall switching in a bistable amplifier was used. Various approximate models were tried for the transmission line and a comparison was made. The line-amplifier model was verified experimentally using a commercially available flip flop.

---

[1] Numbers in brackets refer to bibliography.

CHAPTER II

LITERATURE SURVEY

Transmission Lines

Numerous problems involving signal and power transmission in fluid lines have emerged in the field of fluidics. Although a complete description of dynamic behaviour of a fluid line is extremely difficult, a number of approximate descriptions are available which yield rather good results for engineering design purposes.

Two general approaches to modeling transmission lines have been employed in fluid system analysis [3, 4, 5]:

(1) Lumped Parameter Models

(2) Distributed Parameter Models

The lumped parameter model is valid whenever the time required for a pressure wave to travel the length of the line is short with respect to the period of the highest frequency wave that is to be transmitted. In case where the pressure wave input to the line contains a broad band of frequencies (e.g., step and pulse inputs), a distributed parameter model must be used to achieve acceptable accuracy.

Distributed parameter models are obtained by solving the equations of motion under varying degrees of approximations.

(i) Lossless Model. The lossless model does not include dissipation or heat transfer and hence it yields pure time delay.

(ii) Linear Friction Model. The linear friction model assumes that losses are proportional to mean velocity and heat transfer effects are negligible.

(iii) Constant R-L-C Model. The constant R-L-C model accounts for attenuation only and is valid for cases where the frequency is low and the length to diameter ratio is large.

(iv) Dissipative Model. The dissipative model takes into account the viscous and heat transfer effects and is termed the "Exact Model" [7].

The distributed parameter models can be identified in terms of two functions--the propagation operator, $\Gamma(s)$, and the characteristic impedance, $Z_c(s)$; s is the Laplace variable. These functions result from the solution of a set of equations chosen to describe the line. Brown [7] has obtained expressions for $\Gamma(s)$ and $Z_c(s)$ which are given in the analysis which follows. The exact model does not allow easy computation because of the complex nature of $\Gamma(s)$ and $Z_c(s)$. To overcome this difficulty, many approximations have been suggested in the literature. In this thesis only two will be considered. They are:

(a.) Goodson's Rational Approximation

(b.) Brown's High Frequency Approximation

These will be discussed in detail in the analysis.

Bistable Amplifier

The bistable wall attachment amplifier is essentially a (turbulent) jet confined in a geometry like that illustrated in Figure 1. The jet, in the stable mode, reattaches to one of the two walls due to the Coanda effect. The jet may be switched from one stable mode to another, i.e., from reattaching to one wall to the opposite wall, by the application of a proper control signal. This control signal usually takes the form of a control flow introduced into the control port.

Epstein [1, 2] studied the switching mechanism in a bistable wall attachment fluid amplifier. Depending on the particular geometry of the amplifier, three basic types of switching phenomena can occur (Fig. 2). Of the three, two depend on the length of attachment walls and their offset and the third on the location of the splitter.

End Wall Switching

With relatively short attachment walls, large offset and/or jets with a relatively small control to supply jet momentum ratio, E_1 (see equation 11), the reattachment point, moves downstream until it reaches the edge k of the vent. The jet then separates from the wall, travels across the amplifier and finally reattaches to the opposite wall. For this type of switching to occur it is also necessary to have the splitter located far enough away from the nozzle exit so that it does not interfere with the jet before it separates from the original

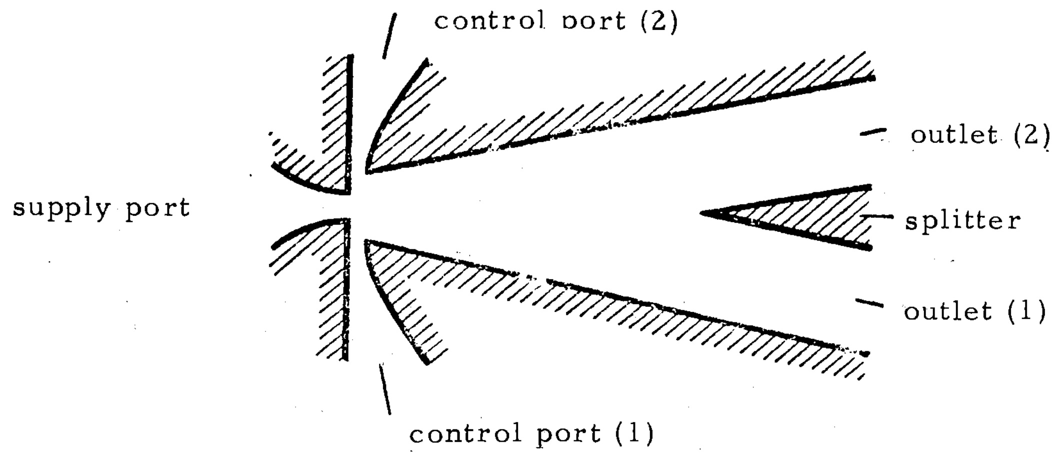

a.) Schematic of an Unvented Bistable Fluid Amplifier

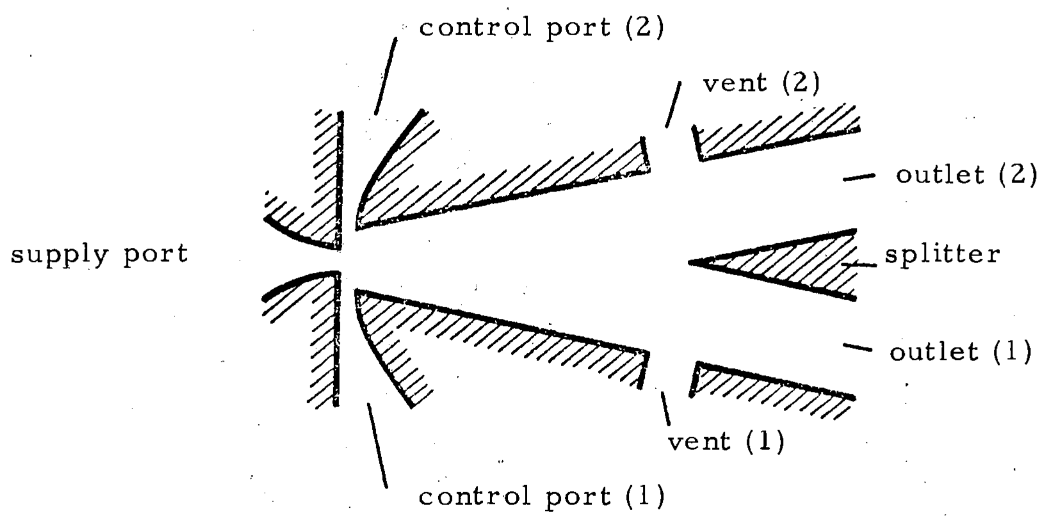

b. Schematic of a Vented Bistable Fluid Amplifier

Figure 1. Schematic of an Unvented and a Vented Bistable Fluid Amplifier

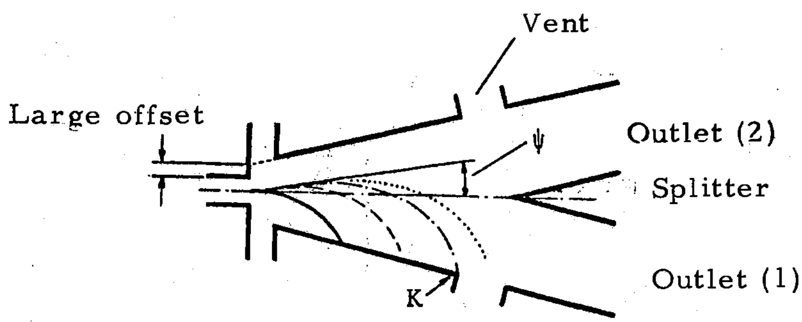

a.) End Wall Switching

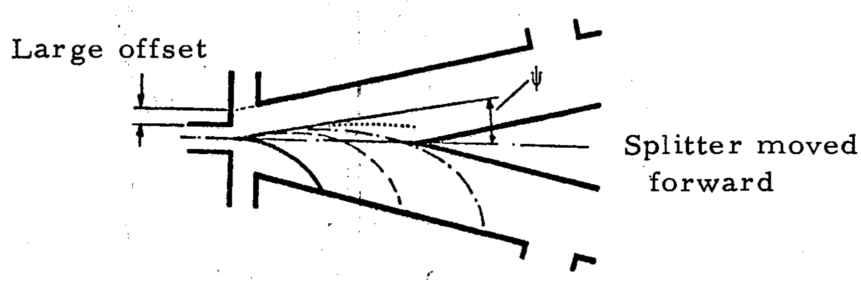

b.) Splitter Switching

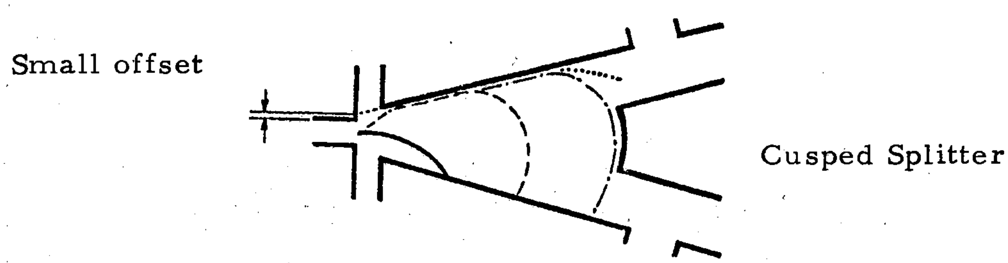

c.) Opposite Wall Switching

Figure 2. Jet Path During the Switching Transient

wall.

Splitter Switching

If the splitter location is as shown in Fig. 2(b), switching occurs when the reattachment point moves downstream a sufficient distance to cause instability of the jet about the splitter leading edge.

Opposite Wall Switching

With relatively small offset and/or large control to supply jet momentum ratio, E_1, the jet attaches to the opposite wall immediately after the control flow is started. The jet, however, still remains attached to the original wall. The two reattachment points move down the amplifier until the flow enters the second outlet. This type of switching is illustrated in Fig. 2(c).

Epstein analyzes only the end wall type switching transient. He divides the end wall switching transient into three phases:

Phase I. Begins when a step input in the control fluid flow is applied and ends when the jet deflection angle, ψ, (see equation 10) reaches its stable value ψ_{final} corresponding to the final control to supply jet momentum ratio, E_1. During this phase the attachment point is assumed to remain at its original position.

Phase II. Follows Phase I and ends when the reattachment point reaches the edge of the vent. During this phase $\psi = \psi_{final}$ = constant.

Phase III. Follows Phase II and ends when a pressure signal is obtained in the receiver connected to the outlet (2) of the amplifier. During this phase $\psi = \psi_{final}$ = constant and the jet is no longer attached to wall (1).

CHAPTER III

ANALYSIS

Transmission Line

A fluid transmission line can be represented in general by a four terminal element having two inputs and two outputs. One particular case is shown below:

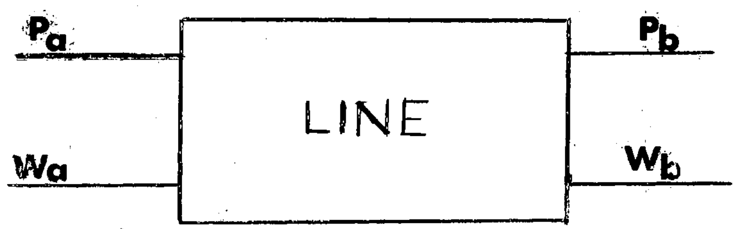

P_a and P_b are pressures and W_a and W_b are mass flow rates. The arrows indicate the causality of the variables, i.e., P_a and W_b are independent variables and W_a and P_b are dependent variables.

The relation between pressures and flows is given by the matrix equation (1):

$$\begin{bmatrix} P_b(s) \\ W_b(s) \end{bmatrix} = \begin{bmatrix} \operatorname{Cosh} \Gamma(s) & -Z_c(s) \operatorname{Sinh} \Gamma(s) \\ -\frac{1}{Z_c(s)} \operatorname{Sinh} \Gamma(s) & \operatorname{Cosh} \Gamma(s) \end{bmatrix} \begin{bmatrix} P_a(s) \\ W_a(s) \end{bmatrix} \quad (1)$$

where $\Gamma(s)$ is termed the propogation operator and $Z_c(s)$ is termed the characteristic impedance.

Brown [7] has derived expressions for $\Gamma(s)$ and $Z_c(s)$ for the case of a pneumatic transmission line and suggested approximations for the high frequency range. The expressions given by Brown are:

$$\Gamma(s) = T_e s \left[\frac{1 + \dfrac{2(\gamma - 1)\, J_1(y)}{yJ_0(y)}}{1 - \dfrac{2\, J_1\,(x)}{x\, J_0\,(x)}} \right]^{1/2}$$

and

$$Z_c(s) = \frac{Z_0}{\left[\left(1 + \dfrac{2(\gamma - 1)J_1(y)}{yJ_0\,(y)}\right) \left(1 - \dfrac{2\, J_1(x)}{x\, J_0(x)}\right) \right]^{1/2}}$$

where

$$y = j\sqrt{\frac{\sigma s r_0^2}{\nu_0}} \; ; \quad x = j\sqrt{\frac{s r_0^2}{\nu_0}} \; ; \quad Z_0 = \frac{C_0}{a}$$

For a line loaded with a linear resistor of impedance, Z_R, the relation between P_b and W_b is

$$P_b(t) = Z_R\, W_b(t) \tag{2}$$

or in terms of the Laplace variable, s,

$$P_b(s) = Z_R\, W_b(s) \tag{3}$$

From equations (1) and (3), $P_b(s)$ can be expressed as a function of $P_a(s)$ as shown below:

$$P_b(s) = \frac{P_a(s)}{\left[\text{Cosh}\,\Gamma(s) + \frac{Z_c(s)}{Z_R}\,\text{Sinh}\,\Gamma(s)\right]}.$$

If $P_a(t)$ is a step input of amplitude, P_a, then

$$P_a(s) = \frac{P_a}{s}$$

$$\frac{P_b(s)}{P_a} = \frac{1}{s\left[\text{Cosh}\,\Gamma(s) + \frac{Z_c(s)}{Z_R}\,\text{Sinh}\,\Gamma(s)\right]} \tag{4}$$

The inverse transform of equation (4) is difficult to obtain due to the complex forms of $\Gamma(s)$ and $Z_c(s)$. A closed form solution can be obtained if approximations are used for $\Gamma(s)$ and $Z_c(s)$. Three approximations are considered below.

Brown's Approximation

For high frequencies or short transient times, $\Gamma(s)$ and $Z_c(s)$ can be approximated by [7]

$$\Gamma(s) \approx T_e s\left[1 + A\left(\frac{1}{ks}\right)^{1/2} + B\left(\frac{1}{ks}\right) + C\left(\frac{1}{ks}\right)^{3/2}\right]$$

and

$$Z_c(s) \approx \frac{Z_0}{\left[1 + D\left(\frac{1}{ks}\right)^{1/2} + E\left(\frac{1}{ks}\right) + F\left(\frac{1}{ks}\right)^{3/2}\right]}$$

where, for liquids,

$$A = 1, \; B = 1, \; C = 7/8$$

$$D = 1, \; E = 0, \; F = 0.13$$

and for gases,

$$A = 1.478, \; B = 1.078, \; C = 1.058$$

$$D = -0.52, \; E = -0.88, \; F = 0.64$$

For sufficiently high frequencies, the fourth terms in the above expressions for $\Gamma(s)$ and $Z_c(s)$ may be neglected. With this additional simplification the inverse transform of equation (4) for the liquids case is:

$$\frac{P_b(t)}{P_a} = 2 \exp\left(\frac{-BT_e}{k}\right) \operatorname{erfc}\left(\frac{1}{2}\sqrt{\frac{T_1}{(t - T_e)}}\right) U_s(t - T_e)$$

$$- 2 \exp\left(\frac{-3BT_e}{k}\right) \operatorname{erfc}\left(\frac{1}{2}\sqrt{\frac{T_2}{(t - 3T_e)}}\right) U_s(t - 3T_e)$$

$$- \frac{2Z_0}{Z_R} \exp\left(\frac{-BT_e}{k}\right) \exp\left(\frac{D^2(t - T_e)}{k} + \sqrt{\frac{D^2 T_1}{k}}\right)$$

$$\operatorname{erfc}\left(\sqrt{\frac{D^2(t - T_e)}{k}} + \frac{1}{2}\sqrt{\frac{T_1}{(t - T_e)}}\right) U_s(t - T_e)$$

$$+ \frac{6Z_0}{Z_R} \exp\left(\frac{-3BT_e}{k}\right) \exp\left(\frac{D^2(t - 3T_e)}{k} + \sqrt{\frac{D^2 T_2}{k}}\right)$$

$$\operatorname{erfc}\left(\sqrt{\frac{D^2(t - 3T_e)}{k}} + \frac{1}{2}\sqrt{\frac{T_2}{(t - 3T_e)}}\right) U_s(t - 3T_e)$$

$$- \frac{6Z_0}{Z_R} \exp\left(\frac{-5BT_e}{k}\right) \exp\left(\frac{D^2(t - 5T_e)}{k} + \sqrt{\frac{D^2 T_3}{k}}\right)$$

$$\operatorname{erfc}\left(\sqrt{\frac{D^2(t - 5T_e)}{k}} + \frac{1}{2}\sqrt{\frac{T_3}{(t - 5T_e)}}\right) U_s(t - 5T_e)$$

$$+ \frac{2Z_0}{Z_R} \exp\left(\frac{-7BT_e}{k}\right) \exp\left(\frac{D^2(t - 7T_e)}{k} + \sqrt{\frac{D^2 T_4}{k}}\right)$$

$$\operatorname{erfc}\left(\sqrt{\frac{D^2(t - 7T_e)}{k}} + \frac{1}{2}\sqrt{\frac{T_4}{(t - 7T_e)}}\right) U_s(t - 7T_e) \qquad (5)$$

where

$$U_s(t - T) = \begin{cases} 0 \text{ for } t < T \\ 1 \text{ for } t > T \end{cases}$$

$$T_1 = \frac{T_e^2 A^2}{k}; \quad T_2 = 9T_1; \quad T_3 = 25T_1; \quad T_4 = 49T_1$$

for the liquid case.

Rational Approximation [8, 9]

Oldenburger and Goodson [9] have shown that the hyperbolic functions of equation (4) can be expanded into the following infinite product forms:

$$\text{Cosh}\,\Gamma(s) = \prod_{n=0}^{\infty}\left[1 + \frac{4\Gamma^2(s)}{(2n+1)^2\pi^2}\right]$$

$$\text{Sinh}\,\Gamma(s) = \Gamma(s)\prod_{n=1}^{\infty}\left[1 + \frac{\Gamma^2(s)}{(n\pi)^2}\right]$$

where

$$\Gamma(s) = \frac{T_e s}{\left[1 - \frac{2J_1(x)}{xJ_0(x)}\right]^{1/2}}$$

The identity

$$J_1(x) = \frac{x}{2}\left[J_0(x) + J_2(x)\right]$$

gives the result:

$$\left[1 - \frac{2J_1(x)}{xJ_0(x)}\right] = -\frac{J_2(x)}{J_0(x)}$$

Infinite product expansions for $J_0(x)$ and $J_2(x)$ are

$$J_0(x) = \prod_{n=1}^{\infty}\left[1 - \frac{x^2}{\alpha^2_{0,n}}\right] = \prod_{n=1}^{\infty}\left[1 + \frac{ks}{\alpha^2_{0,n}}\right]$$

$$J_2(x) = \frac{x^2}{8}\prod_{n=1}^{\infty}\left[1 - \frac{x^2}{\alpha^2_{2,n}}\right] = -\frac{ks}{8}\prod_{n=1}^{\infty}\left[1 + \frac{ks}{\alpha^2_{2,n}}\right]$$

Thus:

$$-\frac{J_2(x)}{J_0(x)} = \frac{\frac{ks}{8}}{\prod_{n=1}^{\infty}\left[\frac{1 + \frac{ks}{\alpha^2_{0,n}}}{1 + \frac{ks}{\alpha^2_{2,n}}}\right]}$$

where $\alpha_{i,n}$ stand for the roots of the equation

$$J_i(\alpha_{i,n}) = 0; \quad n = 1, 2, \ldots; \quad i = 0, 1, 2, \ldots$$

Goodson [8, 9] has found that a good approximation to the infinite products which contain the Bessel function zeros is

$$\prod_{n=1}^{\infty}\left[\frac{1 + \frac{ks}{\alpha^2_{0,n}}}{1 + \frac{ks}{\alpha^2_{2,n}}}\right] = \frac{(1 + P_1 s)(1 + P_2 s)}{(1 + P_3 s)} \quad \text{for } |ks| < 400 \tag{6}$$

where

$$P_1 = \frac{k}{5.78}; \quad P_2 = \frac{k}{56.6}; \quad P_3 = \frac{k}{40.9}$$

Thus:

$$\Gamma^2(s) = \frac{T_e^2 s^2}{\left[1 - \frac{2J_1(x)}{xJ_0(x)}\right]} = \frac{\frac{8T_e^2 s}{k}(1 + P_3 s)}{(1 + P_1 s)(1 + P_2 s)}$$

With this approximation, equation (4) can be rewritten as

$$\frac{P_b(s)}{P_a} = \frac{M(s)}{N(s)}$$

where M(s) and N(s) are polynomials in s of powers of m and n respectively.

The time domain solution can be obtained by the application of the expansion theorem [10] and can be written as

$$\frac{P_b(t)}{P_a} = \frac{M(0)}{N(0)} + \sum_{i=1}^{n} \frac{M(s_i)}{s_i \frac{d}{ds_i}\{N(s_i)\}} \qquad (7)$$

where s_i are given by the roots of the equation

$$N(s_i) = 0$$

Equation (7) was evaluated for n = 0, 1, 2, 3, 4.

Rational Approximation Extended to Pneumatic Case

Using the same expressions for Cosh $\Gamma(s)$ and Sinh $\Gamma(s)$ as given earlier, $\Gamma^2(s)$ for the pneumatic case becomes

$$\Gamma^2(s) = \frac{\dfrac{8T_e^2 s}{k}\left[\gamma - (\gamma - 1)\dfrac{\sigma k s}{8}\,\dfrac{1}{\prod_{n=1}^{\infty}\left[\dfrac{1 + \dfrac{\sigma k s}{\alpha_{0,n}^2}}{1 + \dfrac{\sigma k s}{\alpha_{2,n}^2}}\right]}\right]}{\prod_{n=1}^{\infty}\left[\dfrac{1 + \dfrac{k s}{\alpha_{0,n}^2}}{1 + \dfrac{k s}{\alpha_{2,n}^2}}\right]} \tag{8}$$

where σ is the Prandtl number and γ is the ratio of specific heats. The numerator of equation (8) on the right side containing the zeros of the Bessel function can be approximated by

$$\prod_{n=1}^{\infty}\left[\frac{1 + \dfrac{\sigma k s}{\alpha_{0,n}^2}}{1 + \dfrac{\sigma k s}{\alpha_{2,n}^2}}\right] = \frac{(1 + \sigma P_1 s)(1 + \sigma P_2 s)}{(1 + \sigma P_3 s)} \quad \text{for } |\sigma k s| < 400 \tag{9}$$

The denominator of equation (8) is the same as given in equation (6). Therefore

$$\Gamma^2(s) = \frac{\frac{8T_e^2 s(1+P_1 s)(1+P_2 s)}{k}\left[\gamma(1+\sigma P_1 s)(1+\sigma P_2 s)-\frac{(\gamma-1)\sigma k s}{8}(1+\sigma P_3 s)\right]}{(1+\sigma P_1 s)(1+\sigma P_2 s)(1+P_3 s)}$$

Using this approximation for $\Gamma^2(s)$, the time domain solution for equation (4) can be obtained in the smae way as described earlier. Equation (7) was evaluted for n = 0, 1, 2. Higher values of n were not considered due to computational difficulties.

Bistable Amplifier

The Epstein model (see figure 2(a)) may be used to obtain the switching time of the bistable amplifier. To include line dynamics effects on the switching time, it is necessary to modify the Phase I of the Epstein model.

In Epstein's work, Phase I begins when a step input pressure is applied to the transmission line and ends when the jet deflection angle, ψ, reaches its final value, ψ_{final}, corresponding to the maximum value of the jet momentum ratio, E_1. It is assumed that the jet deflection angle, ψ, as measured at the point of interaction of supply and control jet is given by

$$\psi = \tan^{-1}(E_1) \tag{10}$$

where

$$E_1 = \frac{J_c}{J_s} \tag{11}$$

It is assumed that the control jet total momentum, J_c, is given by

$$J_c = \frac{W_b^2}{\rho b_c d_p} + p_{bubble} b_c d_p, \qquad (12)$$

and the supply jet momentum is

$$J_s = \frac{W_s^2}{\rho b_s d_p} \qquad (13)$$

Since W_b is a function of time, J_c and ψ are functions of time. Knowing $P_b(t)$, $W_b(t)$ can be determined. Hence $\psi(t)$ can be determined. It is assumed that the test amplifier loads the line as if it were a linear resistance, i.e., the input resistance of the amplifier is Z_R as implied by equation (2). A suitable value for Z_R can be determined from a measured pressure-flow characteristic for the amplifier control input port. A measured input characteristic for the test amplifier used is shown in Figure 3; the input resistance is approximately constant.

Phases II and III are not altered since, in accordance with the assumptions of Epstein, $\psi = \psi_{final}$ = constant and hence W_b is constant, corresponding to the switching pressure, P_{sw}.

Switching Time Prediction

The objective of this thesis was to determine the effect of line dynamics on the <u>switching time</u> of a fluidic bistable amplifier.

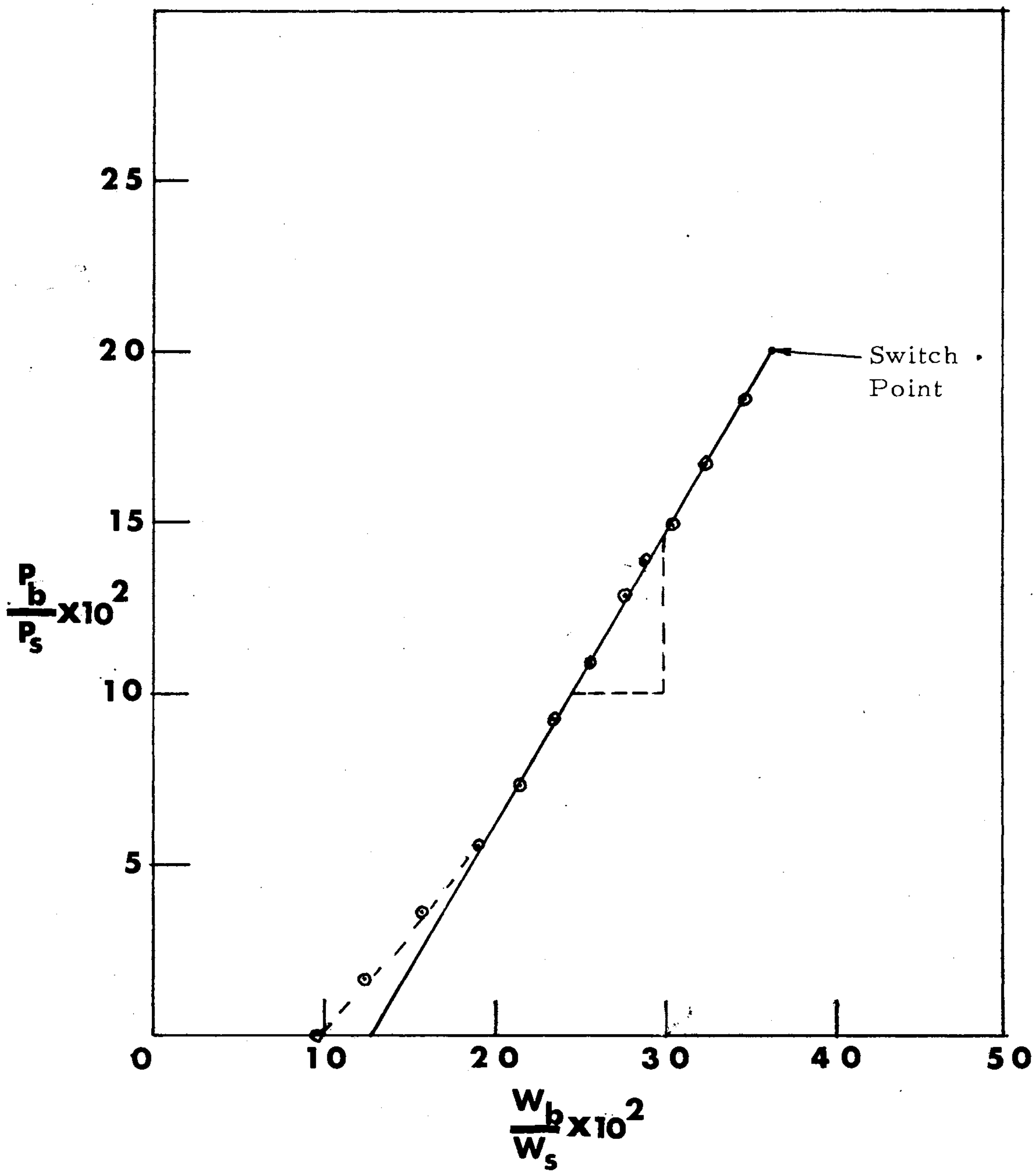

Figure 3. Input Characteristic of the Bistable Amplifier

Switching time is defined here as the time elapsed, beginning with the time of introduction of a step input at the upstream end of the line and commencing with the time when the pressure in the output leg of the bistable amplifier reaches 95% of its final value, less the transport delay.

Figure 4 is a computer flow chart which describes the steps required to predict the switching time for the line-amplifier system, when a step input (approximate) is provided to the line.

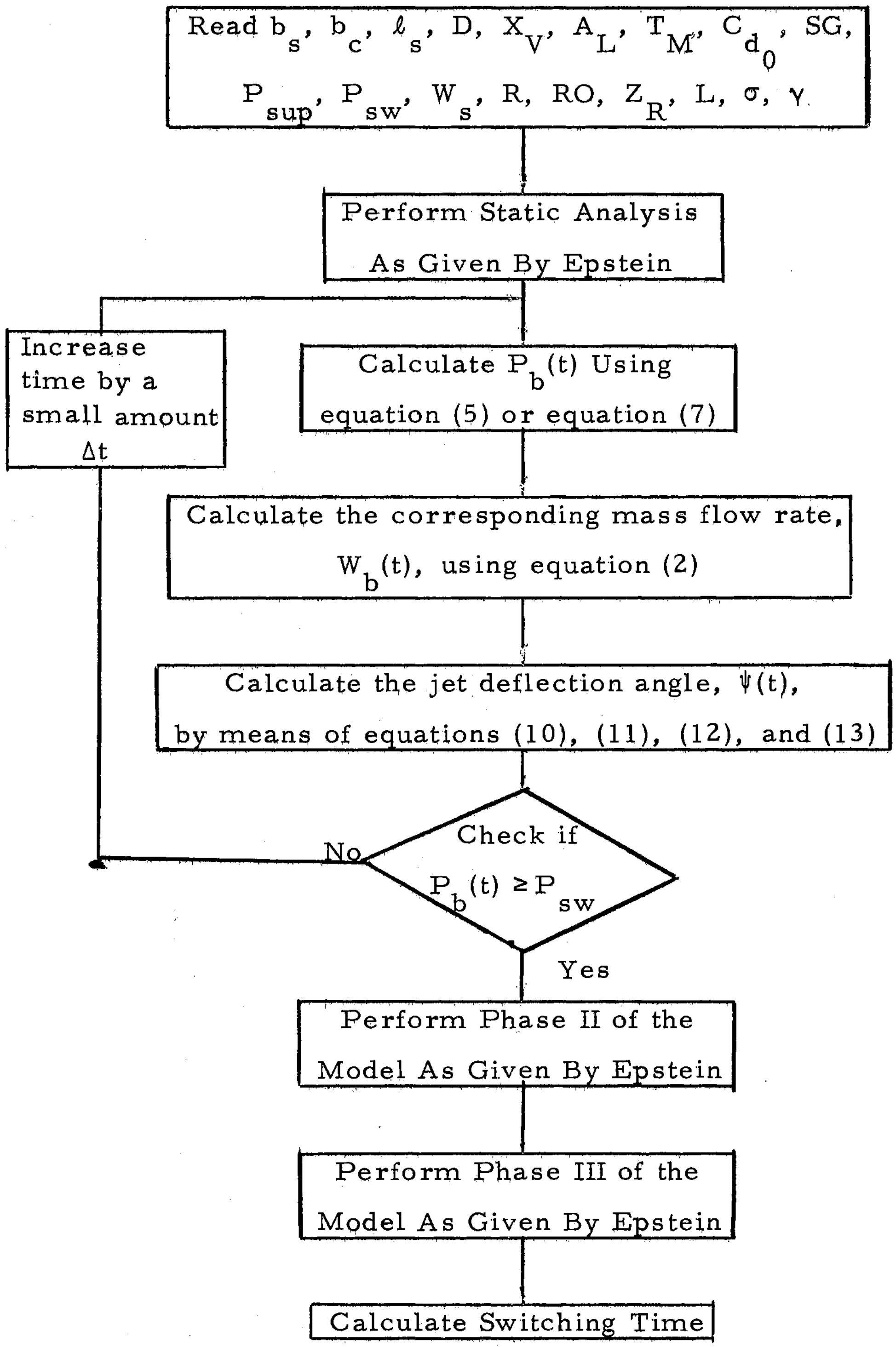

Figure 4. Flow Chart For Computing the Switching Time of the Line-Amplifier System

CHAPTER IV

EXPERIMENTAL APPARATUS AND TECHNIQUE

Figure 5 shows a schematic of the experimental apparatus used. A transmission line connected an output leg of an input amplifier to a control input port of a test amplifier. Both amplifiers were Corning model 190424 bistable flip-flops. Table I gives the dimensions of both amplifiers.

A "step input" to the line was generated by causing the input amplifier output to "switch" from O_2 to O_1. This technique produced a step input having a rise time[1] of approximately 2 msec (msec means millisecond). Attempts to generate a "step" having a rise time less than 2 msec were unsuccessful. Each output leg of the test amplifier was loaded by a control port (resistance) of a similar amplifier.

The supply pressure, P_{s2}, was held constant at 2 psig for all tests. Dynamic pressure measurements were made at the entrance to the line (P_a), the exit of the line (P_b), and the 01 outlet of the test amplifier (P_{01}). All dynamic pressures were measured with Kistler

---

[1] Rise time is defined as the time required for the pressure signal to change from 5 percent to 95 percent of its final value.

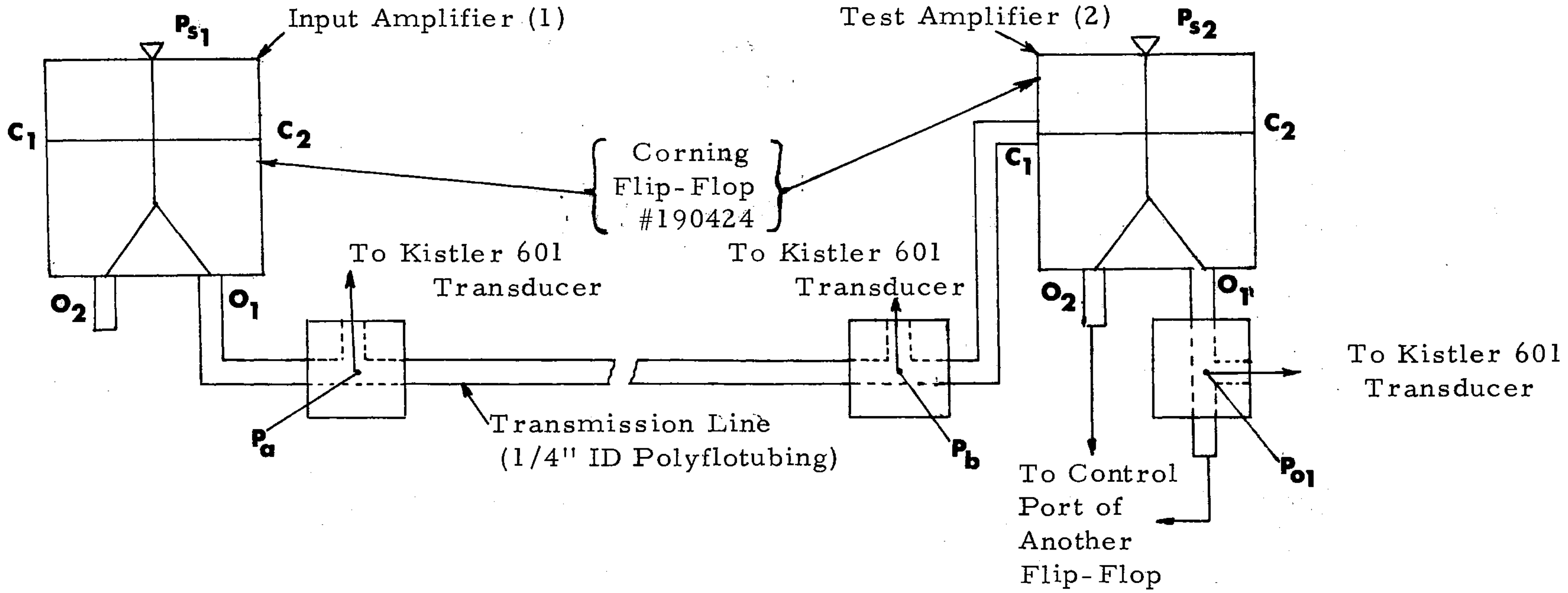

Figure 5. Schematic Diagram of Experimental Setup

model 601 piezoelectric transducers and associated signal conditioning equipment. The step input amplitude was approximately 0.4 psi above atmospheric pressure for all tests. Permanent recordings were made using a storage oscilloscope and camera.

TABLE I

DIMENSIONS OF THE CORNING FLIP-FLOP #190424

Supply Port Nozzle Width	b_s = 0.02 in.
Control Port Nozzle Width	b_c = 0.02 in.
Vent Location	X_V = 0.184 in.
Splitter Location	ℓ_s = 0.22 in.
Wall Angle	A_L = 12°
Wall Offset	D = 0.010 in.
Depth of Amplifier	d_p = 0.08 in.
Vent Discharge Coefficient [1]	C_{d_o} = 0.65
Jet Spread Parameter [1]	SG = 31.5
Maximum Possible Jet Turning Angle [1]	T_M = 67°

Compressed air was used for all measurements. Fluid properties in the line were determined at room temperature and atmospheric pressure.

CHAPTER V

RESULTS AND DISCUSSION

This chapter presents predicted and measured step responses for a pneumatic transmission line terminated by a linear resistor of impedance, Z_R. The effect of input pulse characteristics on the switching time of a bistable amplifier is demonstrated.

Figure 6 shows the calculated step responses for the transmission line loaded at its downstream end with a linear fixed resistance, based on the rational approximate line model with no heat transfer effect (equation 7). There is a marked improvement in the result as the order of approximation (n) is increased. The larger rise time for smaller values of n is a result of neglecting high frequency terms.

In the present work, the rational approximate line model was extended to include heat transfer effects (equation 7). The step response for the line computed using the extended rational approximate model is shown in Figure 7. Computational difficulties prohibited considering values of n greater than 2. In this case also an improvement in the result was observed by increasing n.

It is of interest to examine the importance of heat transfer

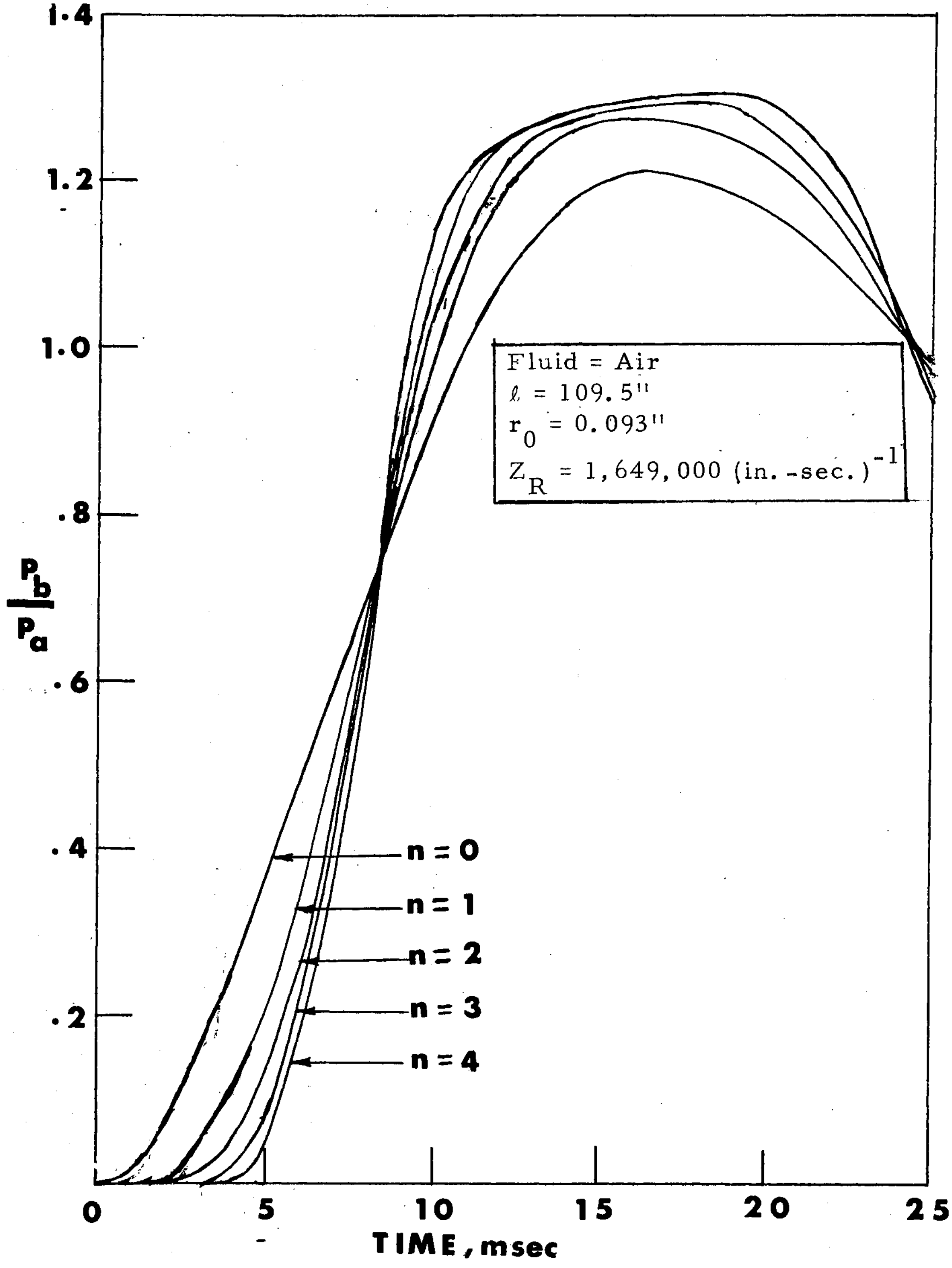

Figure 6. Computed Step Responses of a Pneumatic Transmission Line Terminated With a Linear Resistance--Rational Approximate Model With No Heat Transfer

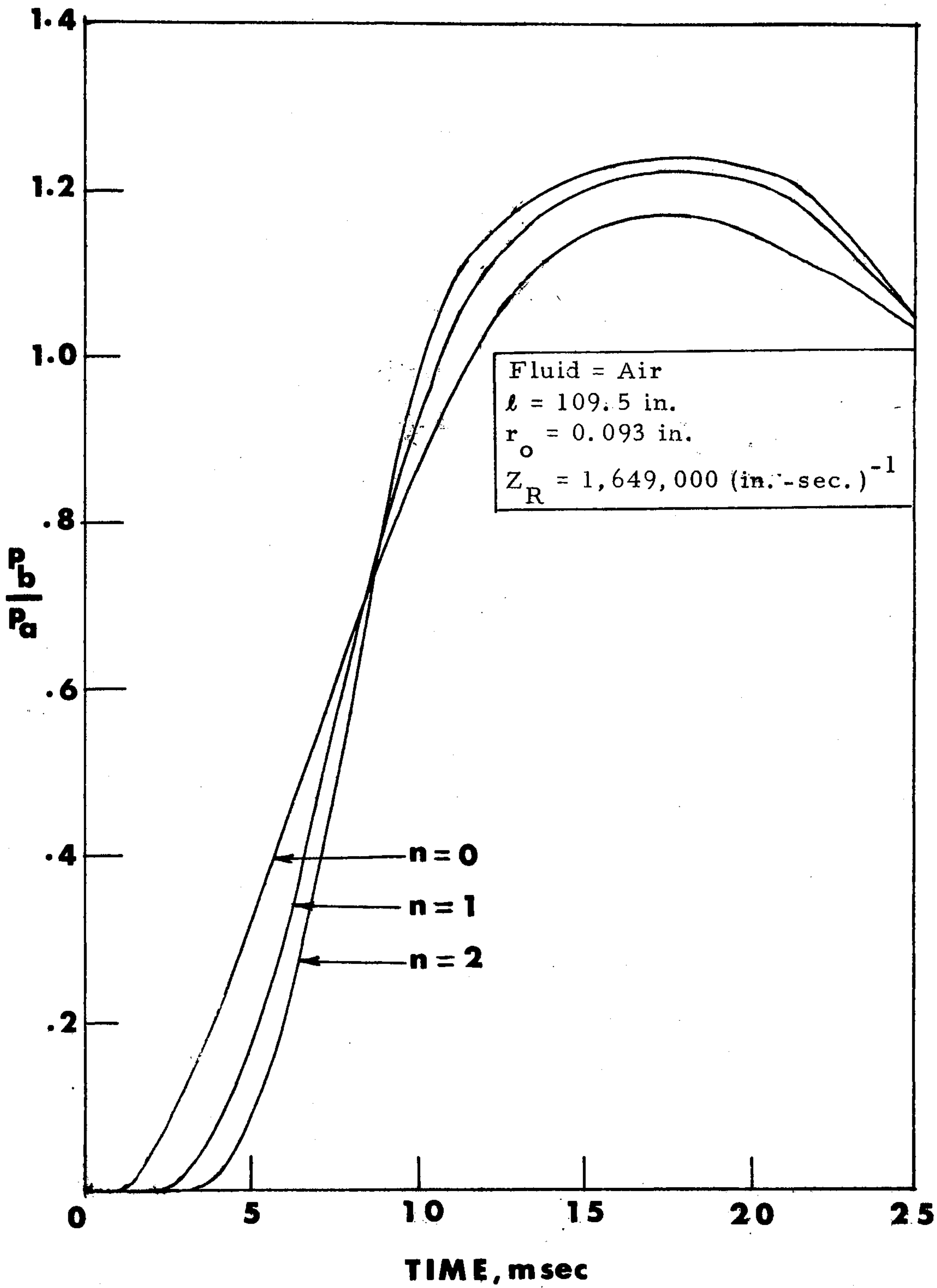

Figure 7. Computed Step Responses of a Pneumatic Transmission Line Terminated With a Linear Resistance--Extended Rational Approximate Model With Heat Transfer

effects on the line dynamics. Step responses calculated using the rational approximate models for n = 2 are shown in Figure 8. For the range of conditions considered, it can be concluded that the heat transfer effects are small.

Figure 9 is a replot of the n = 4 step response from Figure 6 on an extended time scale. A steady state value was reached around 80 msecs.

An experimental study was carried out to provide a means for making a qualitative assessment of the validity of the theoretical predictions and to permit determination of the effect of line dynamics on the switching time of the bistable amplifier. Figure 10 through 13 show measured step responses for the transmission line loaded by a bistable amplifier, having an input resistance of $Z_R = 1,649,000 \text{ (in-sec)}^{-1}$.

Figure 10 shows that the input transient rise time is of the order of 2 msec. There is no response at the downstream end of the line (b end) until an elapsed time of 8 msecs which corresponds to the transport delay. After this, there is a sudden rise which is followed by a slow rise until steady state is reached. The effective rise time is about 10 msecs.

Figure 11 expands the time scale of the lower trace of Figure 10, so that more accurate value of the rise time can be determined.

Figures 13 and 14 show measured responses for a line length of 77 in., and Figure 15 shows the measured response for line length of

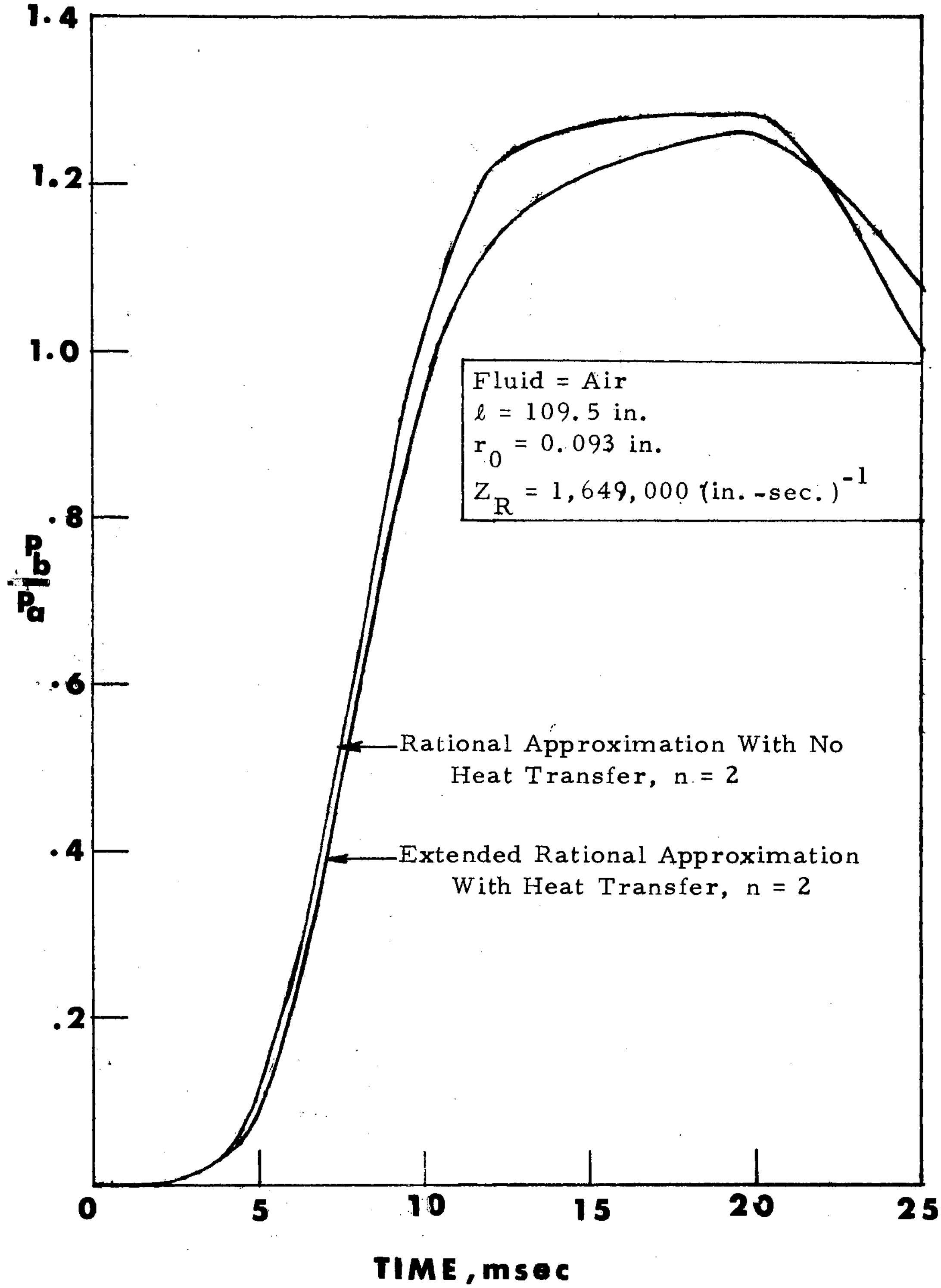

Figure 8. Comparison of the Rational Approximate Models

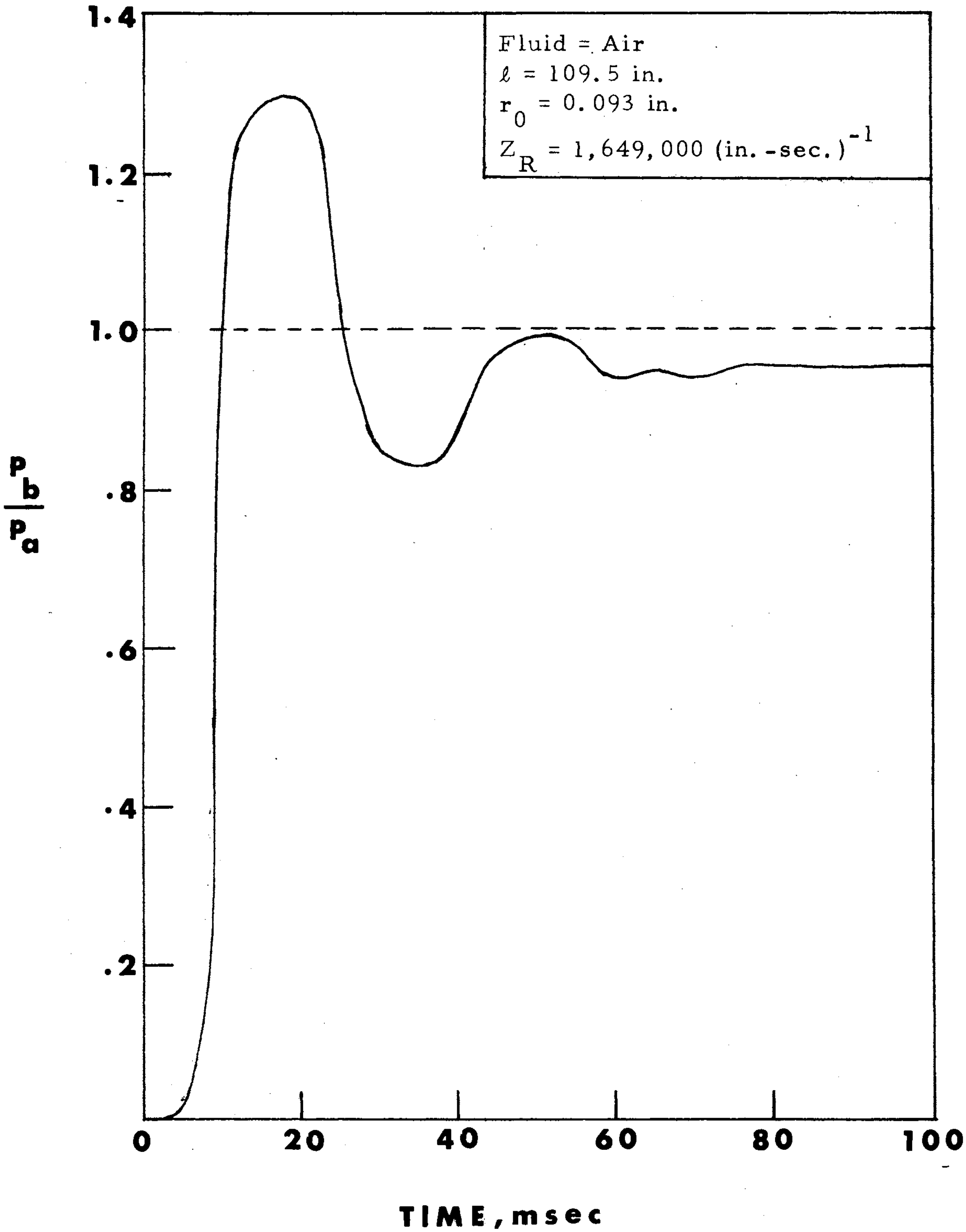

Figure 9. Computed Step Response of a Transmission Line--Rational Approximate Model With No Heat Transfer and n = 4

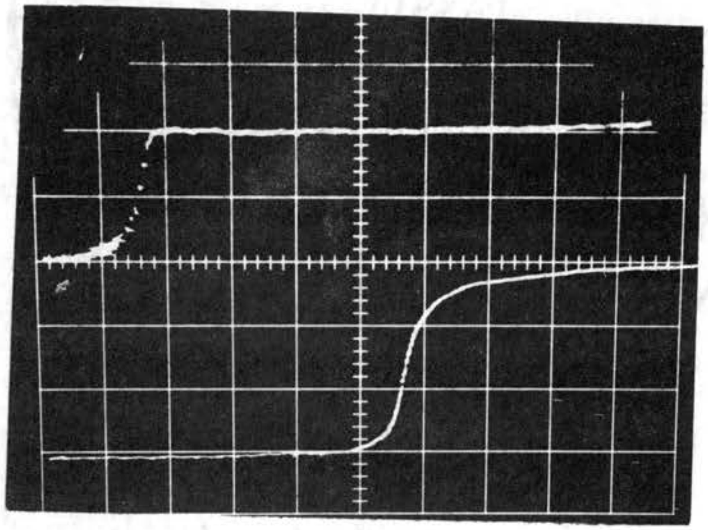

Scale: X--1 unit = 2 msecs.
Y--1 unit = 0.2 psig.
P_s = 2 psig.

Figure 10. Experimental Step Response of a Transmission Line (length = 109.5 in.)

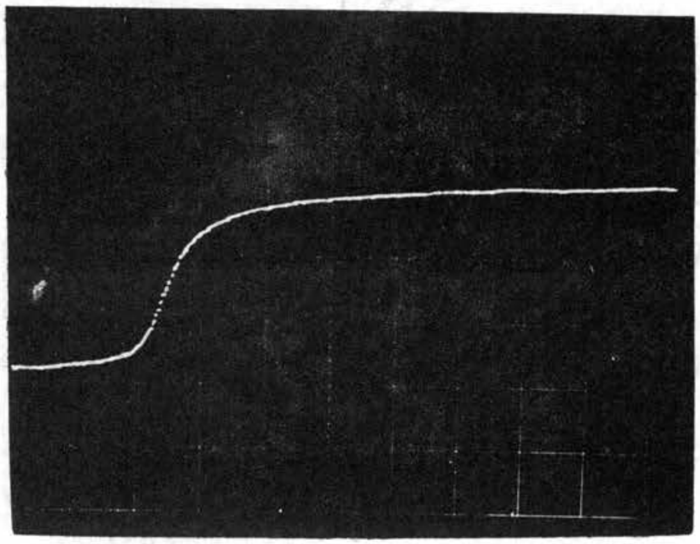

(b) $P_b(t)$

Scale: X--1 unit = 1 msec.
Y--1 unit = 0.2 psig.
P_s = 2 psig.

Figure 11. Experimental Step Response of a Transmission Line (Only Response is Shown) (Line Length = 109.5 in.)

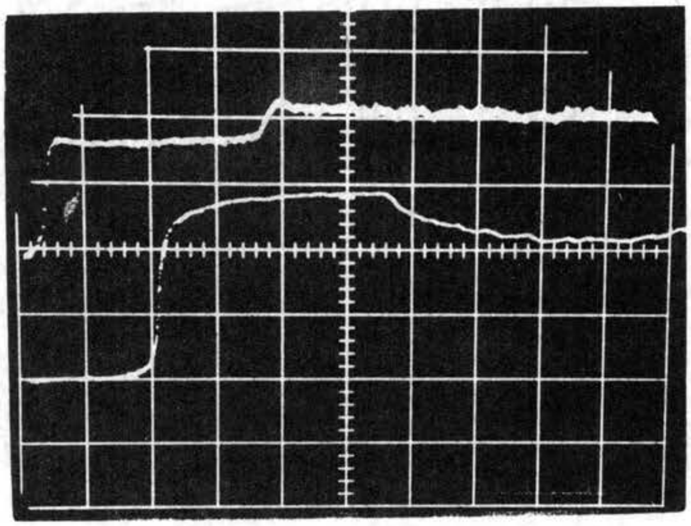

(a) $P_a(t)$

(b) $P_b(t)$

Scale: X--1 unit = 5 msecs.
Y--1 unit = 0.2 psig.
P_s = 2 psig.

Figure 12. Experimental Traces Showing Line Response (Line Length = 109.5 in.)

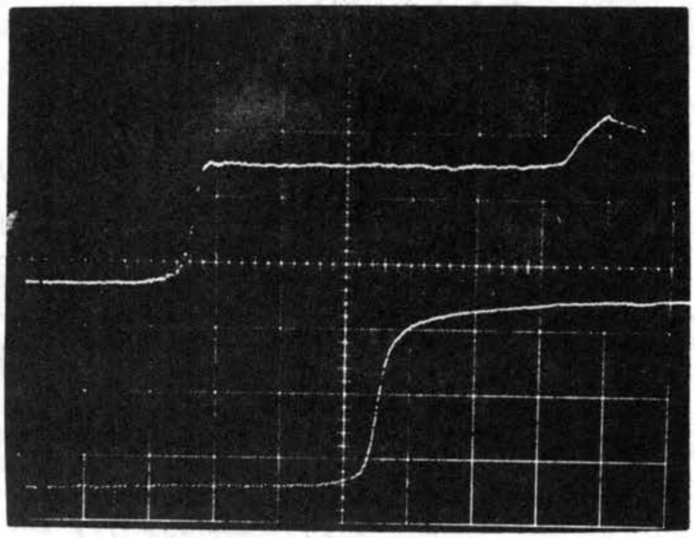

Scale: X--1 unit = 2 msec.
Y--1 unit = 0.2 psig.
P_s = 2 psig.

Figure 13. Experimental Step Response of a Transmission Line (Line Length = 77 in.)

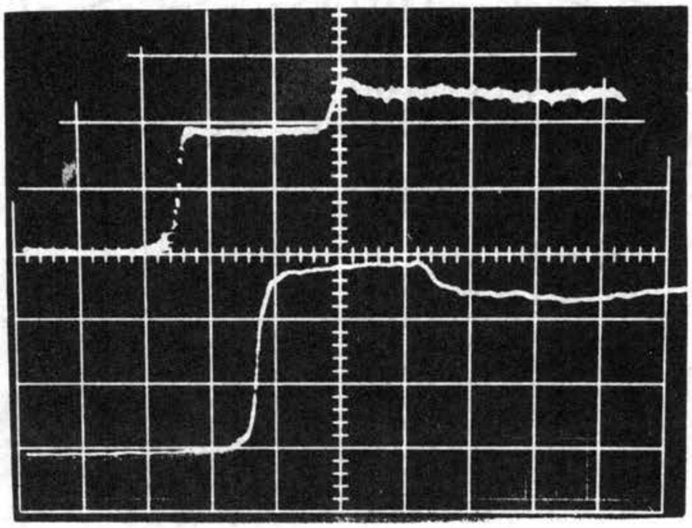

(a) $P_a(t)$

(b) $P_b(t)$

Scale: X--1 unit = 5 msecs.
Y--1 unit = 0.2 psig. (trace (a))
1 unit = 0.2 psig. (trace (b))
P_s = 2 psig.

Figure 14. Experimental Traces Showing Line Response (Line Length = 77 in.)

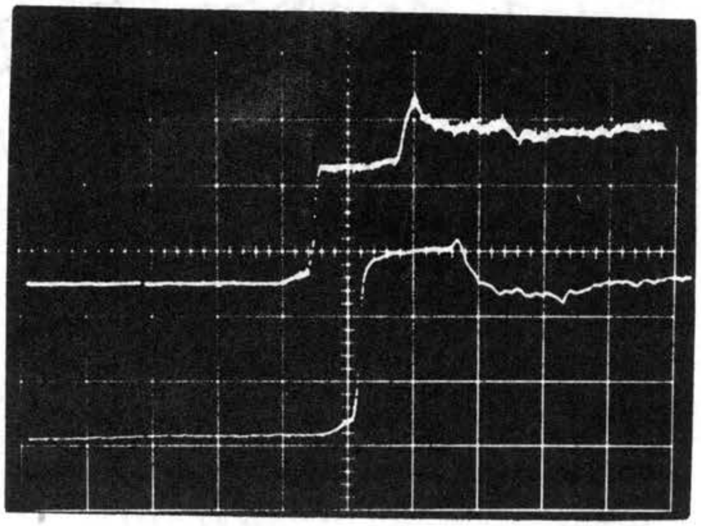

(a) $P_a(t)$

(b) $P_b(t)$

Scale: X--1 unit = 5 msec.
Y--1 unit = 0.2 psig.
P_s = 2 psig.

Figure 15. Experimental Traces Showing Line Response (Line Length = 44 in.)

44 in. The behaviour is similar to that for the longer line.

The step response of a transmission line computed using Brown's high frequency approximation (without heat transfer effects-equation 5) is shown in Figure 16. The approximation is valid for an elapsed time of 40 msecs. Also shown in Figure 16 is a step response of a transmission line computed using the rational approximate model (without heat transfer effects-equation 7) with n = 4. Brown's approximation gives the shortest rise time compared to the rational approximate model. Predictions using the rational approximate model can be improved by increasing the order of approximation, n; however, computational time is accordingly increased. Also shown in Figure 16 are the experimental points obtained from Figure 10. The experimental data correlates well with the predicted results based on Brown's high frequency approximation.

In order to determine the effect of input pulse shape on the switching time of the bistable amplifier, the length of the line was varied and the switching time (see Figure 17) of the amplifier was obtained experimentally and theoretically (using Brown's approximation). The values of switching times for various line lengths are tabulated in Table II.

The experimental switching times were obtained from Figures 18 through 22.

Figure 18 shows measured responses of the line-amplifier system for a line length of 109.5 inches. Trace (a) is the input tran-

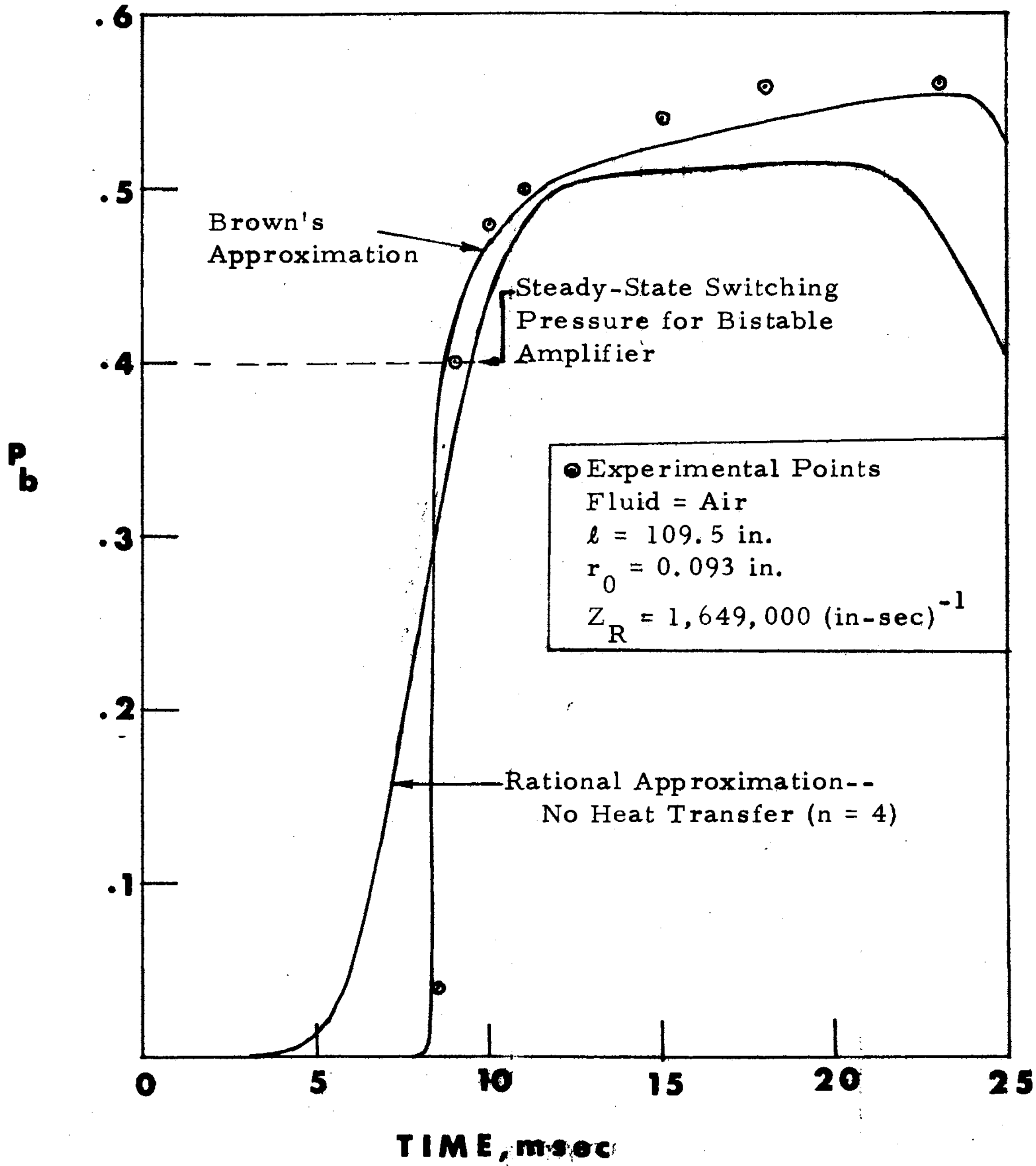

Figure 16. Comparison of Theoretical and Experimental Results for the Step Response of a Transmission Line Terminated by a Linear Resistance

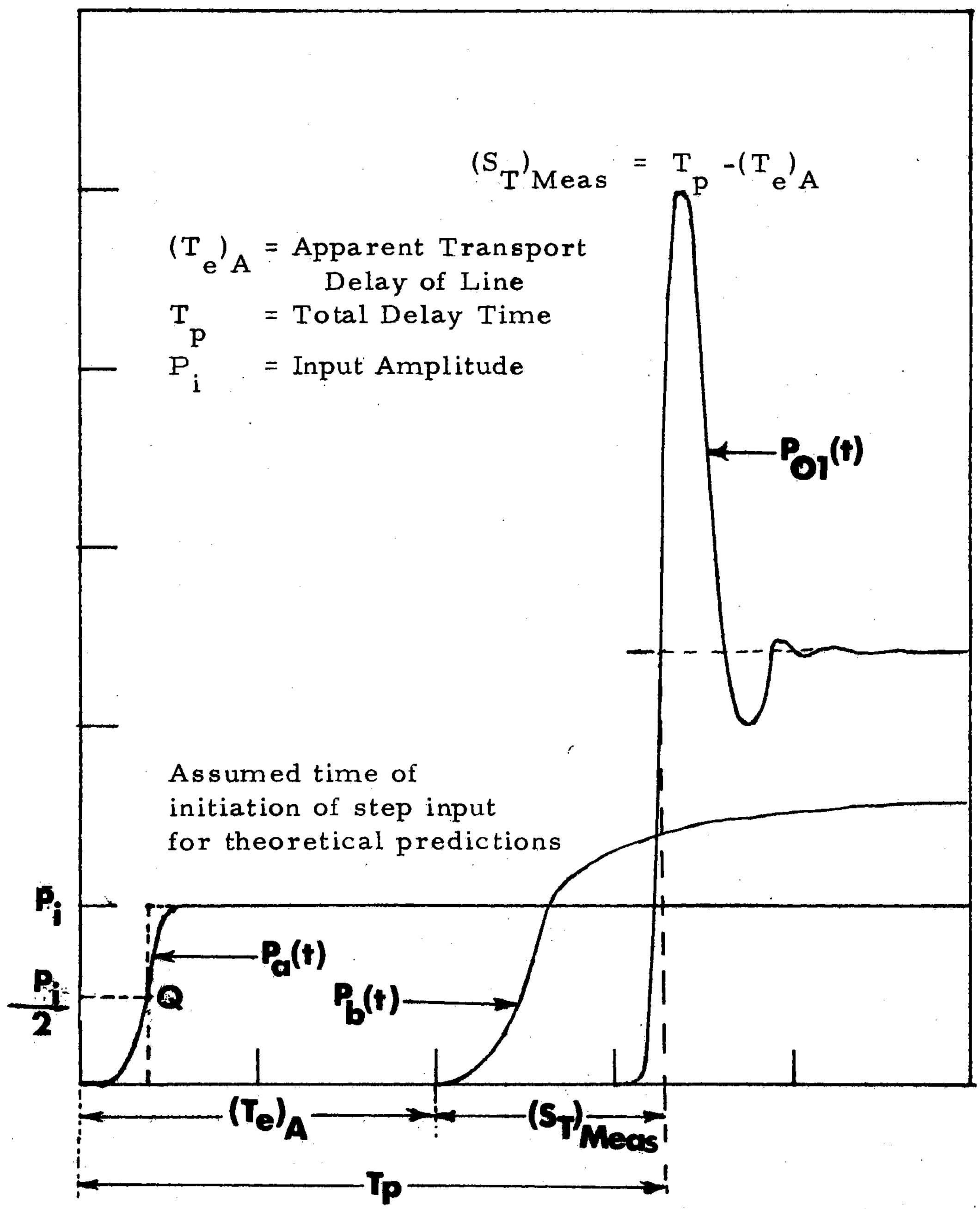

Figure 17. Diagram Defining Experimental Switching Time

TABLE II

EFFECT OF LINE LENGTH ON SWITCHING TIME

S. No.	Line Length, in.	Transport Delay, msec	Uncorrected Theoretical Switching Time, msec	Corrected Theoretical Switching Time, msec	Experimental Switching Time, msec
1.	109.5	8.0	5.2	3.6	4.0
2.	77.0	5.6	4.9	3.3	3.4
3.	44.0	3.2	4.4	2.8	2.8
4.	14.5	1.0	--	--	2.6
5.	2.0	0.15	--	--	2.45

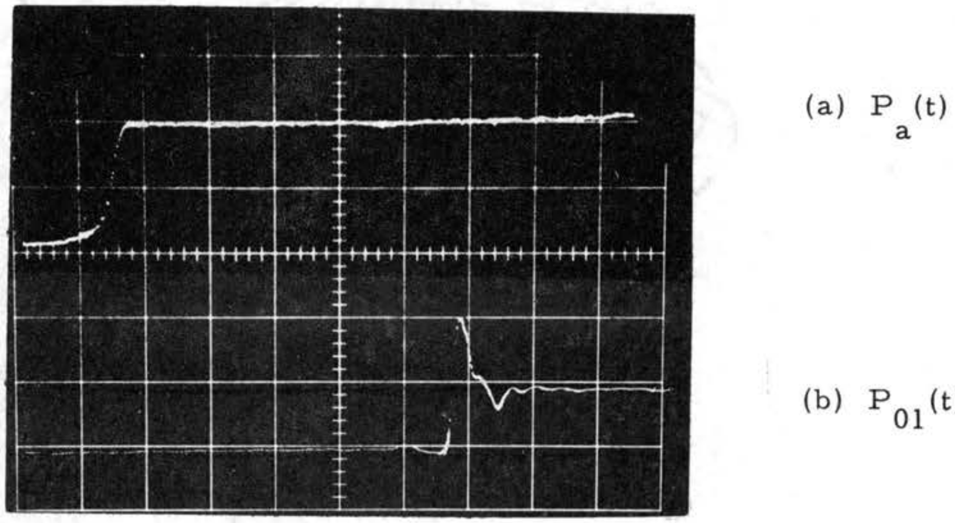

Scale: X--1 unit = 2 msecs.
Y--1 unit = 0.2 psig. (trace (a))
1 unit = 1.0 psig. (trace (b))
P_s = 2 psig.

Figure 18. Experimental Traces for Predicting Switching Time (Line Length = 109.5 in.)

sient at the beginning of the line and trace (b) is the pressure transient at the output leg of the amplifier. The experimental switching time is approximately 4.0 msecs (see Figure 17 for the method of determining the switching time). The uncorrected (see later discussion) theoretical switching time for this case was found to be 5.2 msecs using Brown's approximation for the line.

Figures 19 and 20 show measured responses of the line-amplifier system for line lengths of 77 in. and 44 in. respectively. The corresponding experimental switching times are 3.4 msecs and 2.8 msecs. The uncorrected theoretical switching times using Brown's approximation for the line are 4.9 msecs and 4.4 msecs respectively for the 77 in. and 44 in. lines.

Figures 21 and 22 show measured responses of the line-amplifier system for line lengths of 14.5 in. and 2 in. respectively. The corresponding experimental switching times are 3.6 msecs and 3.0 msecs.

Since the input to the line was not an ideal step, it is necessary to correct the theoretical switching times. A least square fit to the measured input to the line can be a straight line passing through the point Q (see Figure 17) which corresponds to 50% of the input amplitude. It was assumed that the time corresponding to the point Q is the correction which has to be subtracted from the uncorrected theoretical switching time in order to have correspondence with the measured input, and measured switching time. This correction was

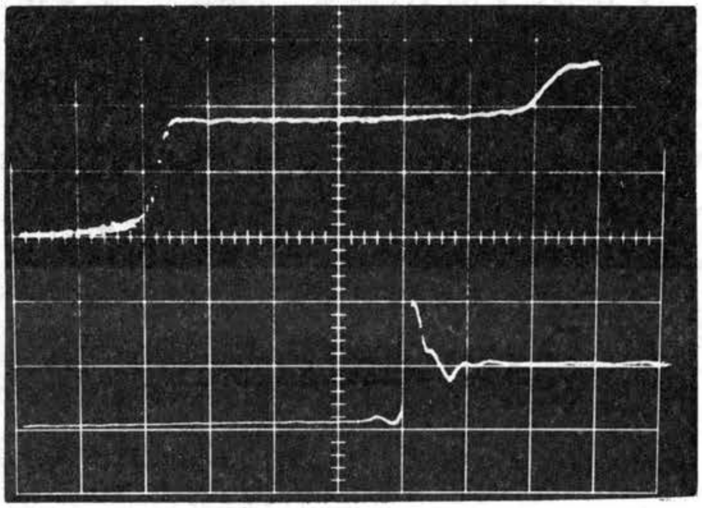

Scale: X--1 unit = 2 msec.
Y--1 unit = 0.2 psig. (trace (a))
1 unit = 1.0 psig. (trace (b))
P_s = 2 psig.

Figure 19. Experimental Traces for Predicting Switching Time (Line Length = 77 in.)

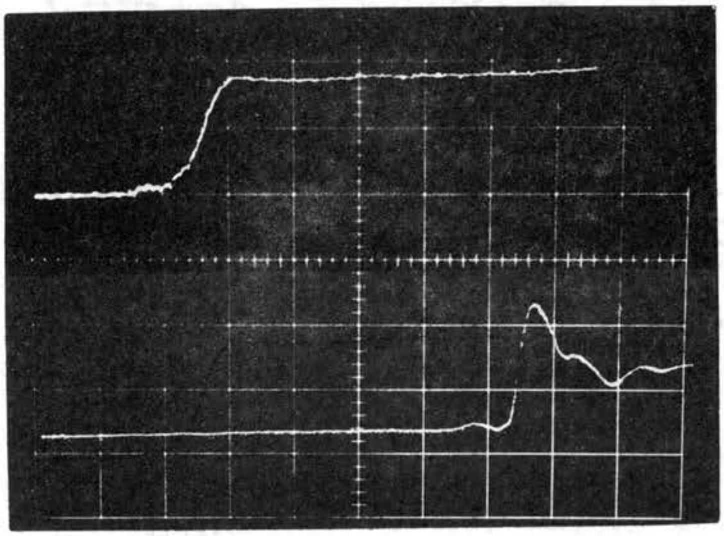

(a) $P_a(t)$

(b) $P_{01}(t)$

Scale: X--1 unit = 1 msec.
Y--1 unit = 0.2 psig. (trace (a))
1 unit = 1.0 psig. (trace (b))
P_s = 2 psig.

Figure 20. Experimental Traces for Predicting Switching Time (Line Length = 44 in.)

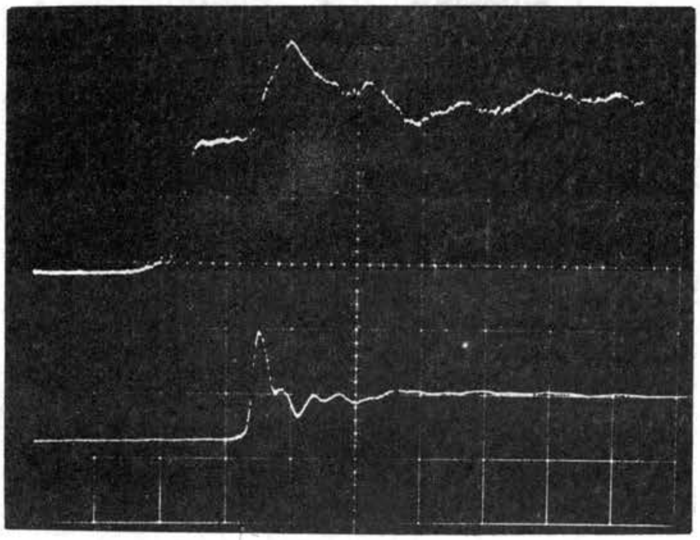

Scale: X--1 unit = 2 msec.
Y--1 unit = 0.2 psig (trace (a))
1 unit = 1.0 psig (trace (b))
P_s = 2 psig.

Figure 21. Experimental Traces for Predicting Switching Time (Line Length = 14.5 in.)

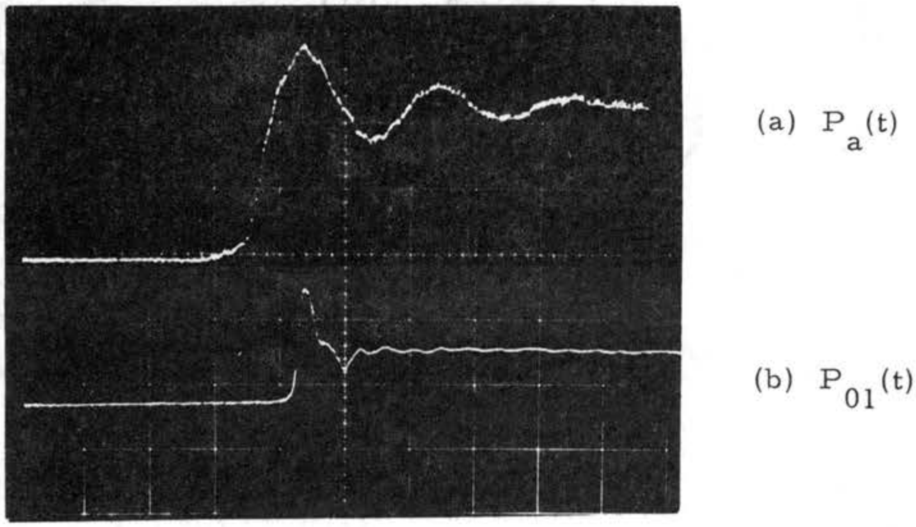

Scale: X--1 unit = 2 msec.
Y--1 unit = 0.2 psig (trace (a))
1 unit = 1.0 psig (trace (b))

Figure 22. Experimental Traces for Predicting Switching Time (line length = 2.0 in.)

found to be of the order of 1.6 msec. The corrected theoretical switching times are 3.6, 3.3, and 2.8 msecs, respectively for line lengths of 109.5 in., 77 in., and 44 in. The corresponding measured switching times are 4.0, 3.4 and 2.8 msecs. Measured switching times for line lengths of 14.5 in., and 2.0 in. are found to be 2.6 and 2.45 msecs, respectively.

Figure 23 shows the plots of measured and predicted switching times versus the line length. As the line length increases, the switching time also increases. At the limiting conditions of zero line length, there remains a time delay of about 2.7 msecs, which accounts for the fundamental dynamics of the bistable amplifiers. The agreement between theory and experiment is good. The theoretical switching time is about 10% less than the measured switching time for a length of 109.5 in. and is less than 1% for line lengths of 77 in. and 44 in. From this it can be concluded that the capacitance effect of the separation bubble is small. Large variation for longer lengths may be due to the larger rise time of the line response.

It is not apparent why the theoretical prediction diverges from the experimental data at small line lengths and as line length increases. The disparity between experiment and theory for small line lengths may be due to complex end effects and reflections.

From Figures 18 through 22 it can be concluded that the rise time of the pressure transient at the outlet leg of the bistable amplifier

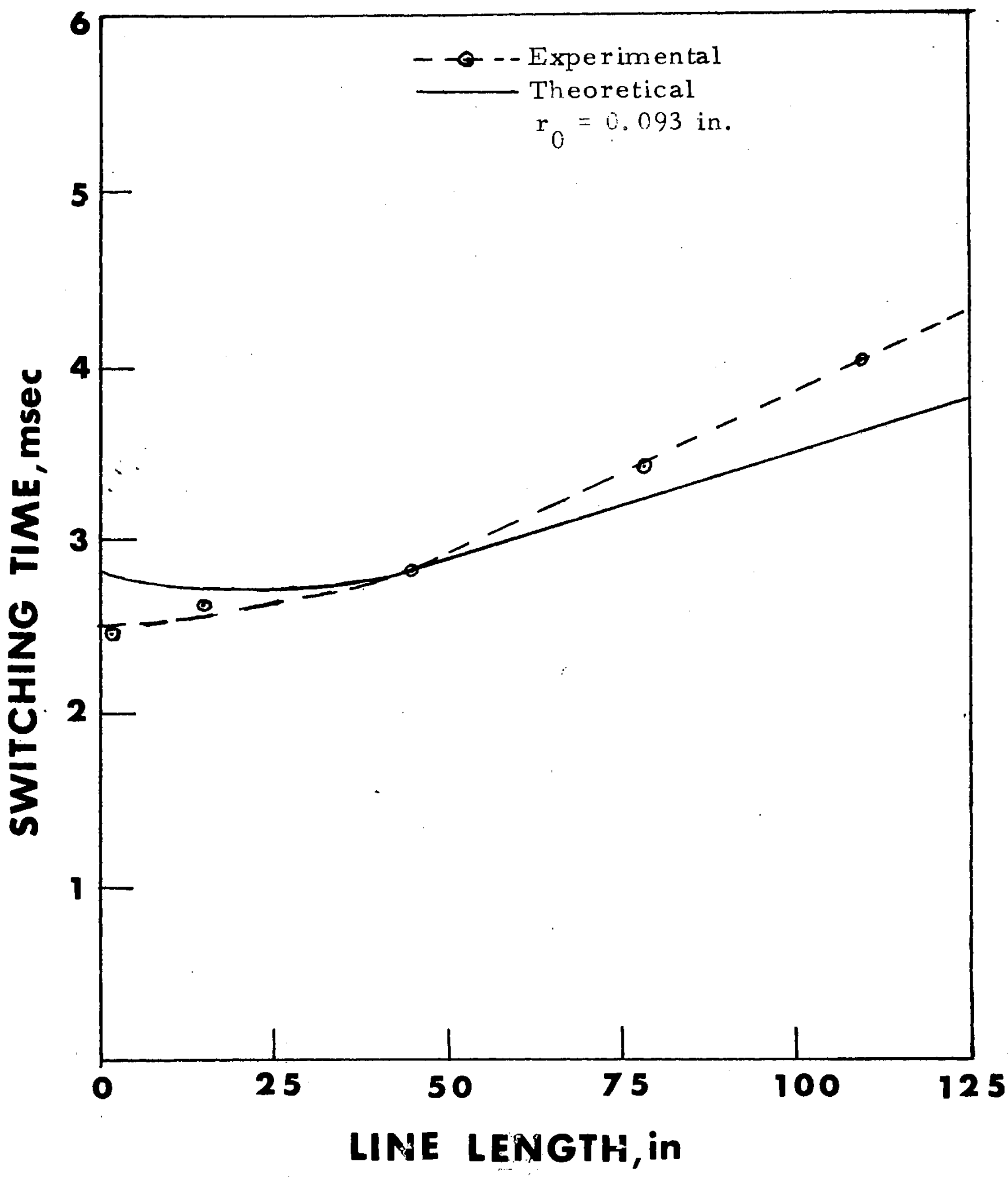

Figure 23. Variation of Switching Time With Line Length

is independent of the input pressure pulse rise of the transmission line.

CHAPTER VI

CONCLUSIONS AND RECOMMENDATIONS

This thesis can be divided into two parts. The first part considered the step response of a pneumatic transmission line terminated by a linear resistance load. Three approximate methods were presented for computing the step response of the line. Of the three approximations evaluated, Brown's high frequency approximation with no heat transfer effects included correlates best with experimental data.

The second part considered the effect of input pulse characteristic on the switching time of a bistable amplifier. A theoretical model was developed for the line-amplifier system by modifying Epstein's model to include line dynamics effects. An experimental verification was carried out using a commercially available bistable amplifier. Two conclusions may be drawn from this study.

Transmission lines of different lengths were used to "produce" different input pulse characteristics. First, there is a significant effect of line dynamics on the switching time of a bistable amplifier. In general, the switching time increases with increases in line length. Second, the rise time of the pressure transient at the output leg of the amplifier is independent of the input pressure pulse shape of the transmission line.

Recommendations for Future Work

The Epstein model is valid for a bistable amplifier with "end-wall switching." Most commercially available amplifiers utilize "opposite-wall switching." The amplifier model of Epstein should be extended to hold for this more common case.

The line model used in the present work was obtained by solving the linearized continuity, momentum, and energy equations and the equation of state. An analysis to extend the linear model to include the nonlinearities will be useful for accurate prediction of line responses.

Also of importance would be extensions of the methods used in this thesis to cases involving other logic elements like the AND element, OR element, NOT element, etc.

BIBLIOGRAPHY

(1) Epstein, M., "Theoretical Investigation of the Switching Mechanism in a Wall Attachment Fluid Amplifier," Ph. D. Thesis, Design Division, Mechanical Engineering Department, Stanford University, Stanford, California, October, 1970.

(2) Epstein, M., "Theoretical Investigation of the Switching Mechanism in a Wall Attachment Fluid Amplifier," ASME Paper No. 70-Flcs-3.

(3) Reid, K. N., "Fluid Transmission Lines," Special Summer Course in Fluid Power Control, Department of Mechanical Engineering, M. I. T., July 1966.

(4) Reid, K. N., "Dynamic Models of Fluid Transmission Lines," Published in the Proceedings of the Symposium on Fluidics and Internal Flows, Pennsylvania State University, October 1969.

(5) Goodson, R. E. and Leonard, R. G., "A Survey of Modeling Techniques for Fluid Line Transients," ASME Paper No. 71-WA/FE-9.

(6) Balakrishna, M., "Step Response of a Pneumatic Transmission Line," A paper presented at the 4th Southwestern Graduate Student Research Conference, Las Cruces, New Mexico, March 23, 24, 1973.

(7) Brown, F. T., "The Transient Response of Fluid Lines," Trans. ASME, J. of Basic Engineering, Series D, Vol, 84, No. 4, December 1962, pp. 547-553.

(8) Reid, K. N., and Brun, R. F., "An Analytical and Experimental Study of a Pulsating Flow Hydraulic System," Report to Allis-Chalmers Mfg. Co., School of Mechanical and Aerospace Engineering, Oklahoma State University, Stillwater, Oklahoma, March 1971.

(9) Oldenburger, R. and Goodson, R. E., "Simplification of Hydraulic Line Dynamics by Use of Infinite Products," Trans. ASME, J. of Basic Engineering, Vol. 86, 1964.

(10) Fodor, G., "Laplace Transforms in Engineering," Akademiai Kiado, Budapest, 1965.

APPENDIX

COMPUTER LISTINGS

```
C    ************************************************************************
C    *                                                                      *
C    *                                                                      *
C    * PROGRAM FOR COMPUTING THE SWITCHING TIME OF A LINE AMPLIFIER MODEL  *
C    *                                                                      *
C    * THE BISTABLE AMPLIFIER IS MODELLED BY MEANS OF THE EPSTEIN MODEL     *
C    *                                                                      *
C    * PHASE-I OF EPSTEIN MODEL IS MODIEFIED TO INCLUDE LINE DYNAMICS       *
C    *                                                                      *
C    * EFFECTS. THE TRANSMISSION LINE CAN BE MODELLED USING ANY ONE OF      *
C    *                                                                      *
C    * THE THREE APPROXIMATIONS.                                            *
C    *                                                                      *
C    * IF ICALL=0, THEN SUBROUTINE RATION IS CALLED. RATION UTILISES THE    *
C    *                                                                      *
C    * RATIONAL APPROXIMATE MODEL WITH NO HEAT TRANSFER EFFECTS.            *
C    *                                                                      *
C    * IF ICALL=1, THEN SUBROUTINE EXTRAT IS CALLED. EXTRAT UTILISES THE    *
C    *                                                                      *
C    * EXTENDED RATIONAL APPROXIMATE MODEL WITH HEAT TRANSFER               *
C    *                                                                      *
C    * IF ICALL=2, THEN SUBROUTINE BROWN IS CALLED. BROWN UTILISES THE      *
C    *                                                                      *
C    * BROWN'S HIGH FREQUENCY APPROXIMATION WITH NO HEAT TRANSFER           *
C    *                                                                      *
C    * THE APPROXIMATION IS VALID ONLY FOR AN ELAPSED TIME OF 40 MSECS      *
C    *                                                                      *
C    * NORDER REFERS TO THE ORDER OF THE APPROXIMATION                      *
C    *                                                                      *
C    * LIBRARY SUBROUTINE POLRT IS USED TO FIND ROOTS OF POLYNOMIAL         *
C    *                                                                      *
C    *                                                                      *
C    ************************************************************************
      DIMENSION ANGLE(200)
      COMMON/GET/ANU,XL,CO,R,ZR,ZETA(200),TIME(200),JJ,WS,PC,NORDER,
     $SI,GA,TO,DT,TMAX
      COMPLEX SUM
      REAL   A,BS,BC,B,BA,CD,D,DI,DII,DW,DD1,DD2,E,EE,F,G,H,JS,JC,J,KB,LS
      REAL   LV,M,PC,RP,RR,RRI,RRP,S,SS,T,V,DV,VW1,VW2,VW3,VW,WS,WC,W,X
      REAL   XV,XVI,X1,DX1,DXA,Z,L,HDFL,DVT,ARG,ARGI,QS
      REAL   AL,RO,PS,PSF,DPS,EP,TM,SG,TRI,DTRI,PRI,BT,GM,TA,DTA,TRII
      REAL   PRII,THI,TPI,DTPI,PPI,LAM,DEL,PY
      REAL    SS4,T4,Y4,K1,RCL,CDO,DEL4
      INTEGER   I,N,K,ICALL,NORDER
    1 READ (5,2) N,K,ICALL,NORDER
    2 FORMAT (4I10)
    3 IF (N.EQ.0) GO TO 999
    4 READ(5,5) BS,BC,XV,LS,D,AL,TM,SG,DEPTH
    5 FORMAT(9F8.4)
 1005 IF (D.LE.0.0) GO TO 897
    6 IF (N.EQ.1) GO TO 15
    7 READ(5,8) RO,WS,PSUP,PO,SI,GA
    8 FORMAT(6F10.7)
      READ(5,76) ANU,CO,R,XL,ZR
   76 FORMAT(5F10.5)
      READ(5,975) TO,DT,TMAX
  975 FORMAT(3F10.6)
   14 GO TO 17
```

G LEVEL 21 MAIN DATE = 73110 22/12/09

```
   15 READ (5,16) EE,M,QS
   16 FORMAT (3F10.5)
   17 IF (AL.LT.TM) GO TO 21
   18 WRITE (6,19) K
   19 FORMAT ('1',20X,'PROBLEM NO.  ',I7,' AL > TM  (IMPOSSIBLE)')
   20 GO TO 1
   21 TA=0.0
   22 PS=0.0
   23 CDO=0.65
  102 PY=3.1415
      RO=RO/(12*12*12)
      AREA=PY*R*R
      ZO=CO/AREA
  103 DTRI=0.05
C ITERATION PROCEDURE FOR DETERMINING THE INITIAL STEADY STATE VALUES
C OF X ,V ,GM AND S.
  104 TRI=(AL+TM)/2.0
  105 EP=(2*TM)/PY
  106 PRI=TRI/EP
  107 ARG=EP*TAN( PRI)
  108 BT=ATAN(ARG)
  109 GM=BT+TRI-AL
  110 ARG1=(GM+PY)/3.0
  111 T=2*COS(ARG1)
  112 S=SG*BS*(1.0/(T*T)-1.0)/3.0
  113 A=S/(0.62*PRI+0.38*SIN(PRI))
  114 RR=A*SIN(PRI)
  115 DW=RR*SIN(TRI-AL)/COS(AL)
  116 DD1=DW-D
  117 IF (ABS(DD1).LT.0.001*D) GO TO 142
  118 TRI=TRI+DTRI
  119 PRI=TRI/EP
  120 ARG=EP*TAN(PRI)
  121 BT=ATAN(ARG)
  122 GM=BT+TRI-AL
  123 ARG1=(GM+PY)/3.0
  124 T=2*COS(ARG1)
  125 S=SG*BS*(1.0/(T*T)-1.0)/3.0
  126 A=S/(0.62*PRI+0.38*SIN(PRI))
  127 RR=A*SIN(PRI)
  128 DW=RR*SIN(TRI-AL)/COS(AL)
  129 DD2=DW-D
  130 IF (ABS(DD2).LT.0.001*D) GO TO 142
  131 IF ((DD1*DD2.GT.0.0).AND.(ABS(DD2).LT.ABS(DD1))) GO TO 134
  132 IF ((DD1*DD2.GT.0.0).AND.(ABS(DD2).GT.ABS(DD1))) GO TO 136
  133 IF (DD1*DD2.LT.0.0) GO TO 139
  134 DD1=DD2
  135 GO TO 118
  136 DD1=DD2
  137 DTRI=-DTRI
  138 GO TO 118
  139 DD1=DD2
  140 DTRI=-0.1*DTRI
  141 GO TO 118
  142 X=RR*COS(TRI)/COS(AL)
  143 V=(A*A*TM/(2.0*PY))*(PRI-0.5*SIN(2.0*PRI))+(D*RR*COS(TRI))/2.0
C END OF ITERATION PROCEDURE
  144 WRITE(6,145)
```

```
  145 FORMAT ('0',8X,'1. INITIAL STEADY STATE RESULTS')
  146 WRITE (6,147)
  147 FORMAT ('0',16X,'TA',8X,'PS',8X,'GM',8X,'DV',6X,'DV/DT',7X,'V',9X,
     1'KB',8X,'X',9X,'H/DEL'//)
  148 WRITE (6,149) TA,PS,GM,V,X
  149 FORMAT (11X,3F10.4,20X,F10.4,10X,F10.4)
      PSW=0.2*PSUP
      JJ=1
      TIME(JJ)=0.0
      ZETA(JJ)=0.0
      ANGLE(JJ)=0.0
      IF (ICALL.EQ.0) GO TO 9998
      IF (ICALL.EQ.1) GO TO 9997
      IF (ICALL.EQ.2) GO TO 9996
 9998 CALL RATION
      GO TO 150
 9997 CALL EXTRAT
      GO TO 150
 9996 CALL BROWN
  150 WRITE (6,151)
  151 FORMAT ('0',8X,'2. BEGINING PHASE 1'//)
      WRITE(6,251)
  251 FORMAT('0',16X,'PC', 7X,'WC', 8X,'TA', 8X,'EE', 8X,'M',/)
      JJ=1
  789 JJ=JJ+1
      PC=ZETA(JJ)
      TA=TIME(JJ)
      IF(PC.LT.0.0) GO TO 778
      GO TO 779
  778 PC=0.0
  779 WC=(PC/(0.741*PSUP)+0.144)*WS
    9 JS=WS*WS*386.4/(RO*BS*DEPTH)
   10 JC=WC*WC*386.4/(RO*BC*DEPTH)
   11 EE=JC/JS
   12 M=WC/WS
   13 QS=WS/RO
  206 PSF=ATAN(EE)
      WRITE(6,250) PC,WC,TA,EE,M
  250 FORMAT(10X,5F10.5)
      ANGLE(JJ)=PSF
      IF (PC.EQ.0.0) GO TO 789
      IF(PC.GE.PSW) GO TO 786
      GO TO 789
  786 PSF=(ANGLE(JJ)+ANGLE(JJ-1))/2.
      TA=(TIME(JJ)+TIME(JJ-1))/2.
      PS=PSF
  207 S=S-BC/2.0
  210 ARG=1.0+TAN(PS)**2
  211 B=BS*(1.0+M)*(1.0+M)/SQRT(ARG)
  212 ARG=1.0+3.0*S/(SG*B)
  213 ARG1=(GM+PY)/3.0
  214 KB=0.5-COS(ARG1)*SQRT(ARG)
  215 BA=B*(1.0-2.0*KB)
  216 DXA=(BC+BA*SIN(PS))/(2.0*COS(AL))
  217 DII=D+DXA*SIN(AL)-(BA*COS(PS)-BS)/2.0
  218 X1=X-DXA
  246 WRITE (6,247)
  247 FORMAT ('0',8X,'3. BEGINING PHASE 2'//)
```



```
      TLINE=TA*1000
      WRITE (6,147)
  300 DX1=(XV-X1-DXA)/25.0
C INCREASING BUBBLE VOLUME USING SMALL INCREMENTS DXI
  301 X1=X1+DX1
  302 L=X1*SIN(AL)
  303 ARG=(L+DII)**2+(X1*COS(AL))**2
  304 RR=SQRT(ARG)
  305 ARG=DII*COS(AL)/RR
  306 TRII=ARSIN(ARG)+PS+AL
  307 PRII=TRII/EP
  308 A=RR/SIN(PRII)
  309 ARG=2.0*PRII
  310 VW1=(A*A*TM/(2.0*PY))*(PRII-0.5*SIN(ARG))
  311 ARG=TRII-PS
  312 VW2=0.5*DII*RR*COS(ARG)
  313 VW3=0.5*DXA*(DII+D)*COS(AL)
  314 VW=VW1+VW2+VW3
  315 IF ((VW-V).LE.0.0) GO TO 301
  316 DTA=(VW-V)/(KB*QS*(1.0+M))
  317 ARG=EP*TAN(PRII)
  318 BT=ATAN(ARG)
  319 GM=BT+TRII-PS-AL
  320 S=A*(0.62*PRII+0.38*SIN(PRII))
  321 ARG=1.0+3.0*S/(SG*B)
  322 ARG1=(GM+PY)/3.0
  323 KB=0.5-COS(ARG1)*SQRT(ARG)
  324 BA=B*(1.0-2.0*KB)
  325 DXA=(BC+BA*SIN(PS))/(2.0*COS(AL))
  326 DII=D+DXA*SIN(AL)-(BA*COS(PS)-BS)/2.0
  327 X=X1+DXA
  328 DV=VW-V
  329 DVT=DV/DTA
  330 V=VW
  331 TA=TA+DTA
  332 WRITE (6,333) TA,PS,GM,DV,DVT,V,KB,X
  333 FORMAT (11X,8F10.4)
  334 IF ((XV-X).LT.(DX1/2.0)) GO TO 337
  335 IF (KB.LT.0.0001) GO TO 900
  336 GO TO 301
  337 WRITE (6,338)
  338 FORMAT ('0',8X,'4. BEGINING PHASE 3'//)
      WRITE (6,147)
  395 ARG=(GM+PY)/3.0
  396 T4=2.0*COS(ARG)
  397 SS4=S+(SG*B)/3.0
 1397 DEL4=1.825*SS4/SG
  398 ARG=(1.0+T4)/(1.0-T4)
  399 Y4=(0.5*SS4*ALOG(ARG))/SG
  400 DX=(BC+B*SIN(PS))/(2.0*COS(AL))
  401 XVI=XV-DX
  402 LV=XVI*SIN(AL)
  403 DI=D+DX*SIN(AL)-(B*COS(PS)-BS)/2.0
 1403 IF (DI.LT.0.0) GO TO 903
  404 ARG=(DI+LV)**2+(XVI*COS(AL))**2
  405 RRI=SQRT(ARG)
  406 ARG=XVI*COS(AL)/RRI
  407 THI=ARCOS(ARG)+PS
```

```
C ITERATION PROCEDURE FOR DETERMINING THE INITIAL PASSAGE WIDTH Z IN PHASE 3
  408 DTPI=0.01
  409 TPI=THI
  410 I=0
  411 TPI=TPI-DTPI
  412 PPI=TPI/EP
  413 ARG=EP*TAN(PPI)
  414 BT=ATAN(ARG)
  415 ARG=THI-TPI
  416 Z=RRI*SIN(ARG)/COS(BT)
  417 ARG=BT+TPI-THI
  418 RP=RRI*COS(ARG)/COS(BT)
  419 A=RP/SIN(PPI)
  420 ARG=2.0*PPI
  421 VW1=(A*A*TM/(2.0*PY))*(PPI-0.5*SIN(ARG))
  422 ARG=THI-TPI
  423 VW2=RP*RRI*SIN(ARG)/2.0
  424 VW3=(DI*XVI+(D+DI)*DX)*COS(AL)/2.0
  425 VW=VW1+VW2+VW3
  426 IF (I.EQ.2) GO TO 437
  427 IF (I.EQ.1) GO TO 433
  428 IF (VW.LT.V) GO TO 411
  429 IF (VW.EQ.V) GO TO 438
  430 DTPI=-0.1*DTPI
  431 I=1
  432 GO TO 411
  433 IF (VW.GT.V) GO TO 411
  434 DTPI=-0.1*DTPI
  435 I=2
  436 GO TO 411
  437 IF (VW.LT.V) GO TO 411
C END OF ITERATION PROCEDURE
  438 DTPI=0.50*(THI-TPI)
C INCREASING BUBBLE VOLUME USING SMALL INCREMENTS DTPI
  439 TPI=TPI-DTPI
  440 PPI=TPI/EP
  441 ARG=EP*TAN(PPI)
  442 BT=ATAN(ARG)
  443 ARG=THI-TPI
  444 Z=RRI*SIN(ARG)/COS(BT)
  445 ARG=BT+TPI-THI
  446 RP=RRI*COS(ARG)/COS(BT)
  447 A=RP/SIN(PPI)
  448 ARG=2.0*PPI
  449 VW1=(A*A*TM/(2.0*PY))*(PPI-0.5*SIN(ARG))
  450 ARG=THI-TPI
  451 VW2=RP*RRI*SIN(ARG)/2.0
  452 VW3=(DI*XVI+(D+DI)*DX)*COS(AL)/2.0
  453 VW=VW1+VW2+VW3
  454 RRP=RP/(2.0*SIN(TPI))
 1454 K1=RRP+B/2.0-Y4
 2454 ARG=2.0*TPI
 3454 RCL=RRP+B/2.0+(0.5*(K1**2-RRP**2))/(RRP*COS(ARG)-K1)
  455 F=RCL*COS(PS)
  456 E=LS-(BC/2.0+RCL*SIN(PS))
  457 ARG=F*F+E*E
  458 G=SQRT(ARG)
  459 H=G-RCL
```



```
  460 ARG=E/F
  461 LAM=ATAN(ARG)
  462 SS=SG*B/3.0+RCL*(PS+LAM)
  463 DEL=1.825*SS/SG
  464 IF (H.LT.(-0.7*DEL)) GO TO 954
 1465 ARG=(-Z/DEL4)
 2465 CD=CD0*(1.0-EXP(ARG))
  466 ARG=2.0/(RCL*B)
  467 KB=CD*Z*SQRT(ARG)
  468 DTA=(VW-V)/(KB*QS*(1.0+M))
  469 DV=VW-V
  470 V=VW
  471 TA=TA+DTA
  472 DVT=DV/DTA
  473 HDEL=H/DEL
  474 WRITE(6,475) TA,PS,GM,DV,DVT,V,KB,X,HDEL
  475 FORMAT (11X,9F10.4)
 1475 IF (I.GE.400) GO TO 894
 2475 I=I+1
  476 GO TO 439
  894 WRITE (6,895)
  895 FORMAT ('0',20X,'TOO CLOSE TO ASYMPTOTE')
  896 GO TO 1
  897 WRITE (6,898)
  898 FORMAT ('0',20X,'D NOT POSITIVE')
  899 GO TO 1
  900 WRITE (6,901)
  901 FORMAT ('0',20X,'KB LESS THAN 0.0001')
  902 GO TO 1
  903 WRITE (6,904)
  904 FORMAT ('0',20X,'DI<0  (IMPOSSIBLE)')
  905 GO TO 1
  954 TA=TA*1000
C INSTRUCTIONS FOR PRINTING AMPLIFIER AND FLOW PARAMETERS DATA
   27 WRITE (6,28) K
   28 FORMAT ('1',6X,' PROBLEM NUMBER',I7)
   29 WRITE (6,30)
   30 FORMAT ('0',6X,' SWITCHING TIME IN BISTABLE WALL ATTACHMENT
     1FLUID AMPLIFIERS  (END WALL SWITCHING TRANSIENT)'///)
      IF(ICALL.EQ.0) GO TO 671
      IF(ICALL.EQ.1) GO TO 672
      IF(ICALL.EQ.2) GO TO 673
  671 WRITE(6,661)
  661 FORMAT('0',18X,'THIS PROGRAM UTILISED THE RATIONAL APPROXIMATE
     $MODEL FOR THE TRANSMISSION LINE WITH NO HEAT TRANSFER EFFECTS',/)
      GO TO 555
  672 WRITE(6,652)
  652 FORMAT('0',18X,'THIS PROGRAM UTILISES THE EXTENDED RATIONAL
     $APPROXIMATE MODEL FOR THE TRANSMISSION LINE WITH HEAT TRANSFER',/)
      GO TO 555
  673 WRITE(6,653)
  653 FORMAT('0',18X,'THIS PROGRAM UTILISED THE BROWN HIGH FREQUENCY
     $APPROXIMATION FOR THE TRANSMISSION LINE WITH NO HEAT TRANSFER',/)
  555 WRITE(6,77)
   77 FORMAT('0',8X,'1. TRANSMISSION LINE DATA:')
      WRITE(6,70) XL
   70 FORMAT('0',8X,'LENGTH OF TRANSMISSION LINE:          XL=',F9.3)
      WRITE(6,71) CD
```

```
   71 FORMAT('0',8X,'ACOUSTIC VELOCITY:            CO=',F8.2)
      WRITE(6,75) R
   75 FORMAT('0',8X,'RADIUS OF THE TRANSMISSION LINE:        R=',F8.6)
   33 WRITE (5,34)
   34 FORMAT ('0',8X,'2.  AMPLIFIER DATA:')
      WRITE(6,664) DEPTH
  664 FORMAT(' ',18X,'DEPTH OF THE AMPLIFIER:              DP=',F9.7)
   35 WRITE (6,36) BS
   36 FORMAT ('0',18X,'SUPPLY PORT WIDTH:                  BS=',F6.3)
   37 WRITE (6,38) BC
   38 FORMAT (' ',18X,'CONTROL PORT WIDTH:                 BC=',F6.3)
   39 WRITE (6,40) XV
   40 FORMAT (' ',18X,'VENT LOCATION:                      XV=',F6.3)
 1040 WRITE (6,2040) CDD
 2040 FORMAT (' ',18X,'VENT DISCHARGE COEFFICIENT          CDD=',F5.3)
   41 WRITE (6,42) LS
   42 FORMAT (' ',18X,'SPLITTER LOCATION:                  LS=',F6.3)
   43 WRITE (6,44) D
   44 FORMAT (' ',18X,'WALL OFFSET:                        D=',F6.3)
   45 WRITE (6,46) AL
   46 FORMAT (' ',18X,'WALL ANGLE:                         AL=',F6.3)
   47 WRITE (6,48)
   48 FORMAT ('0',8X,'3.  FLOW PARAMETERS:')
   49 WRITE (6,50) SG
   50 FORMAT ('0',18X,'JET SPREAD PARAMETER:               SG=',F6.3)
   51 WRITE (6,52) TM
   52 FORMAT (' ',18X,'MAX POSSIBLE JET TURNING ANGLE:     TM=',F6.3)
   53 WRITE (6,54) EE
   54 FORMAT ('0',18X,'C/S JET MOMENTUM RATIO:             E= ',F9.7)
   55 WRITE (6,56) M
   56 FORMAT (' ',18X,'C/S MASS FLOW RATE RATIO:           M= ',F9.7)
   57 WRITE (6,58) QS
   58 FORMAT (' ',18X,'SUPPLY VOLUME FLOW RATE:            QS=',F9.6)
   59 IF (N.EQ.1) GO TO 68
   60 WRITE (6,61) WS
   61 FORMAT ('0',18X,'SUPPLY MASS FLOW RATE:              WS=',F9.7)
   62 WRITE (6,63) WC
   63 FORMAT (' ',18X,'CONTROL MASS FLOW RATE:             WC=',F9.7)
   64 WRITE (6,65) PC
   65 FORMAT (' ',18X,'CONTROL PORT PRESSURE:              PC=',F6.3)
   66 WRITE (6,67) RO
   67 FORMAT (' ',18X,'FLUID DENSITY:                      RO=',F9.7)
      WRITE(6,657) SI
  657 FORMAT(' ',18X,'PRANDTL NUMBER:                      SI=',F9.6)
      WRITE(6,658) GA
  658 FORMAT(' ',18X,'RATIO OF SPECIFIC HEAYS:             GA=',F9.6)
   68 CONTINUE
      WRITE(6,909) TA
  909 FORMAT (/,20X,'SWITCHING TIME=',F8.2,'MILLISECONDS',/,'0')
  955 GO TO 1
  999 RETURN
      END
```



```
      SUBROUTINE RATION
C
C     RATIONAL APPROXIMATE MODEL WITH NO HEAT TRANSFER EFFECTS.
C
      COMPLEX S(50),CMPLX,SUM,D(50),CEXP,AN
      DIMENSION C1(50),C2(50),AA(50)
      DIMENSION XCOF(30),COF(30),ROOTR(30),ROOTI(30)
      COMMON/GET/ANU,XL,CO,R,ZR,ZETA(200),TIME(200),JJ,WS,PO,NORDER,
     $SI,GA,TO,DT,TMAX
      RK=R*R/ANU
      PI=22.0/7.0
      AREA=PI*R*R
      ZO=CO/AREA
      TE=XL/CO
      T1=RK/5.78
      T2=RK/56.6
      T3=RK/40.9
      T1PT2=T1+T2
      T1T2=T1*T2
      N=NORDER
      CALL TRANSA(N,RK,ZO,TE,T1PT2,T1T2,T3,G1,C1,N1,ZR)
      CALL TRANSB(N,RK,ZO,TE,T1PT2,T1T2,T3,G2,C2,N2,ZR)
      DO 40 I=1,N2
      AA(I)=C1(I)*G1+C2(I)*G2
   40 CONTINUE
      AA(N2+1)=C1(N1)*G1
      M=N2
      WRITE(6,254)
  254 FORMAT(15X,'COEFFICIENTS OF POLYNOMIAL IN S IN ASCENDING POWERS')
      DO 50 J=1,N1
      WRITE(6,284) AA(J)
  284 FORMAT(10X,E15.8,/)
      XCOF(J)=AA(J)
   50 CONTINUE
      CALL POLRT(XCOF,COF,M,ROOTR,ROOTI,IER)
      SS=1./XCOF(1)
      WRITE(6,264)
  264 FORMAT(25X,'REAL',35X,'IMAGINARY',/)
      DO 291 I=1,M
      WRITE(6,294) ROOTR(I),ROOTI(I)
  294 FORMAT(20X,E15.8,20X,E15.8,/)
  291 CONTINUE
      T=TO
      TM=TMAX
   60 SUM=(0.0,0.0)
      D(1)=XCOF(2)
      DO 295 I=1,M
      S(I)=CMPLX(ROOTR(I),ROOTI(I))
      DO 300 J=2,M
  300 D(J)=D(J-1)+J*(S(I)**(J-1))*XCOF(J+1)
      AN=(1.0+T3*S(I))
      AN=AN**(N+1)
      SUM=SUM+AN*CEXP(S(I)*T)/(D(M)*S(I))
  295 CONTINUE
      SUM=(SS+SUM)*PO
      JJ=JJ+1
      TIME(JJ)=T
      ZETA(JJ)=SUM
```

```
      WRITE(6,292) SUM,T
  292 FORMAT(20X,E15.8,20X,E15.8,20X,E15.8,/)
      IF (REAL(SUM).GE.PO) RETURN
  298 T=T+DT
      IF(T-TM) 60,60,42
   42 RETURN
      END
```



```
      SUBROUTINE TRANSA(N,RK,ZO,TE,T1PT2,T1T2,T3,GN,CN,NN,ZR)
      DIMENSION CN(20),CD(20),XN(20),XD(20),YN(20),YD(20)
      PIBYTE=22.0/7.0/TE
      CONST=RK/32.0*PIBYTE*PIBYTE
      GN=1.0/CONST
      ND=4
      NN=4
      CN(1)=CONST
      CN(2)=CONST*T3+1.0
      CN(3)=T1PT2
      CN(4)=T1T2
      IF(N.EQ.0) RETURN
      YN(3)=CN(3)
      YN(4)=CN(4)
      DO 30 M=1,N
      TMP1=2*M+1
      C11=CONST*TMP1*TMP1
      YN(1)=C11
      YN(2)=C11*T3+1.0
      GN=GN/C11
      NNX=NN
      DO 10 I=1,NNX
   10 XN(I)=CN(I)
      NDX=ND
      DO 20 I=1,NDX
   20 YD(I)=YN(I)
      CALL PMPY(CN,NN,XN,NNX,YD,NDX)
   30 CONTINUE
      RETURN
      END
```

```
V G LEVEL  21                TRANSB           DATE = 73110           22/12/09

      SUBROUTINE TRANSB(N,RK,ZO,TE,T1PT2,T1T2,T3,GN,CN,NN,ZR)
      DIMENSION CN(20),CD(20),XN(20),XD(20),YN(20),YD(20)
      PIBYTE=22.0/7.0/TE
      CONST=RK/32.0*PIBYTE*PIBYTE
      GN=8.0*TE*ZO/(RK*ZR)
      NN=3
      ND=4
      CN(1)=1.0
      CN(2)=T1PT2
      CN(3)=T1T2
      IF(N.EQ.0) RETURN
      YN(3)=T1PT2
      YN(4)=T1T2
      DO 30 M=1,N
      C12=CONST*M*M*4.0
      YN(1)=C12
      YN(2)=C12*T3+1.0
      GN=GN/C12
      NNX=NN
      DO 10 I=1,NNX
   10 XN(I)=CN(I)
      NDX=ND
      DO 20 J=1,NDX
   20 YD(J)=YN(J)
      CALL PMPY(CN,NN,XN,NNX,YD,NDX)
   30 CONTINUE
      RETURN
      END
```

```
V G LEVEL  21                PMPY             DATE = 73110           22/12/09

      SUBROUTINE PMPY(Z,IDIMZ,X,IDIMX,Y,IDIMY)
      DIMENSION Z(50),X(50),Y(50)
      IDIMZ = IDIMX+IDIMY-1
      DO 30 I=1,IDIMZ
   30 Z(I) = 0.0
      DO 40 I=1,IDIMX
      K = I-1
      DO 40 J=1,IDIMY
      K = K+1
   40 Z(K) = X(I)*Y(J) + Z(K)
      RETURN
      END
```

```
      SUBROUTINE EXTRAT
C
C     EXTENDED RATIONAL APPROXIMATE MODEL WITH HEAT TRANSFER EFFECTS
C
      COMPLEX S(50),CMPLX,SUM,D(50),CEXP,AN,BN,CN
      DIMENSION C1(50),C2(50),AA(50)
      DIMENSION XCOF(30),COF(30),ROOTR(30),ROOTI(30)
      COMMON/GET/ANU,XL,CO,R,ZR,ZETA(200),TIME(200),JJ,WS,PO,NORDER,
     $SI,GA,TO,DT,TMAX
      RK=R*R/ANU
      PI=22.0/7.0
      AREA=PI*R*R
      ZO=CO/AREA
      TE=XL/CO
      T1=RK/5.78
      T2=RK/56.6
      T3=RK/40.9
      T1PT2=T1+T2
      T1T2=T1*T2
      N=NORDER
      CALL TRANSC(N,RK,ZO,TE,T1,T2,T3,G1,C1,N1,ZR,GA,SI)
      CALL TRANSD(N,RK,ZO,TE,T1,T2,T3,G2,C2,N2,ZR,GA,SI)
      DO 40 I=1,N2
      AA(I)=C1(I)*G1+C2(I)*G2
   40 CONTINUE
      AA(N2+1)=C1(N1)*G1
      M=N2
      WRITE(6,254)
  254 FORMAT(15X,'COEFFICIENTS OF POLYNOMIAL IN S IN ASCENDING POWERS')
      DO 50 J=1,N1
      WRITE(6,284) AA(J)
  284 FORMAT(10X,E15.8,/)
      XCOF(J)=AA(J)
   50 CONTINUE
      CALL POLRT(XCOF,COF,M,ROOTR,ROOTI,IER)
      SS=1./XCOF(1)
      WRITE(6,264)
  264 FORMAT(25X,'REAL',35X,'IMAGINARY',/)
      DO 291 I=1,M
      WRITE(6,294) ROOTR(I),ROOTI(I)
  294 FORMAT(20X,E15.8,20X,E15.8,/)
  291 CONTINUE
      T=TO
      TM=TMAX
   60 SUM=(0.0,0.0)
      D(1)=XCOF(2)
      DO 295 I=1,M
      S(I)=CMPLX(ROOTR(I),ROOTI(I))
      DO 300 J=2,M
  300 D(J)=D(J-1)+J*(S(I)**(J-1))*XCOF(J+1)
      AN=(1.0+T3*S(I))
      BN=(1.0+SI*T1*S(I))
      CN=(1.0+SI*T2*S(I))
      AN=AN*BN*CN
      AN=AN**(N+1)
      SUM=SUM+AN*CEXP(S(I)*T)/(D(M)*S(I))
  295 CONTINUE
      SUM=(SS+SUM)*PO
```



```
      JJ=JJ+1
      WRITE(6,292) SUM,T
  292 FORMAT(20X,E15.8,20X,E15.8,20X,E15.8,/)
      TIME(JJ)=T
      ZETA(JJ)=SUM
      IF (REAL(SUM).GE.PO) RETURN
  298 T=T+DT
      IF(T-TM) 60,60,42
   42 RETURN
      END
```

```
      SUBROUTINE TRANSC(N,RK,ZO,TE,T1,T2,T3,GN,CN,NN,ZR,GA,SI)
      COMMON/ALL/PHI1,PHI2,A1,A2,A3,B1,B2
      DIMENSION CN(50),CD(50),XN(50),XD(50),YN(50),YD(50)
      PIBYTE=22.0/7.0/TE
      CONST=RK/32.0*PIBYTE*PIBYTE
      GN=1.0/CONST
      ND=6
      NN=6
      A1=SI*SI*T1*T2*T3
      A2=SI*SI*T1*T2+SI*T3*(T1+T2)
      A3=SI*(T1+T2)+T3
      B1=GA*SI*SI*T1*T2+GA*SI*(T1+T2)*(T1+T2)+GA*T1*T2-(GA-1.0)
     $*SI*RK*(T1+T2+SI*T3)/8.0
      B2=(SI+1.0)*GA*(T1+T2)-(GA-1.0)*SI*RK/8.0
      CN(1)=CONST
      CN(2)=CONST*A3+GA
      CN(3)=CONST*A2+B2
      CN(4)=CONST*A1+B1
      CN(5)=GA*SI*SI*(T1+T2)*T1*T2+GA*SI*(T1+T2)*T1*T2-(GA-1.0)
     $*SI*RK*((T1+T2)*T3*SI+T1*T2)/8.0
      CN(6)=GA*SI*SI*T1*T2*T1*T2-(GA-1.0)*SI*SI*RK*T1*T2*T3/8.0
      IF(N.EQ.0) RETURN
      YN(6)=CN(6)
      YN(5)=CN(5)
      PHI1=YN(6)
      PHI2=YN(5)
      DO 30 M=1,N
      TMP1=2*M+1
      C11=CONST*TMP1*TMP1
      YN(4)=C11*A1+B1
      YN(3)=C11*A2+B2
      YN(2)=C11*A3+GA
      YN(1)=C11
      GN=GN/C11
      NNX=NN
      DO 10 I=1,NNX
   10 XN(I)=CN(I)
      NDX=ND
      DO 20 I=1,NDX
   20 YD(I)=YN(I)
      CALL PMPY(CN,NN,XN,NNX,YD,NDX)
   30 CONTINUE
      RETURN
      END
```



```
      SUBROUTINE TRANSD(N,RK,ZO,TE,T1,T2,T3,GN,CN,NN,ZR,GA,SI)
      COMMON/ALL/PHI1,PHI2,A1,A2,A3,B1,B2
      DIMENSION CN(50),CD(50),XN(50),XD(50),YN(50),YD(50)
      PIBYTE=22.0/7.0/TE
      CONST=RK/32.0*PIBYTE*PIBYTE
      GN=8.0*TE*ZO/(RK*ZR)
      NN=5
      ND=6
      CN(1)=1.0
      CN(2)=(SI+1.0)*(T1+T2)
      CN(3)=(SI*SI*T1*T2+SI*(T1+T2)*(T1+T2)+T1*T2)
      CN(4)=SI*SI*T1*T2*(T1+T2)+SI*T1*T2*(T1+T2)
      CN(5)=SI*SI*T1*T2*T1*T2
      IF(N.EQ.0) RETURN
      YN(6)=PHI1
      YN(5)=PHI2
      DO 30 M=1,N
      C12=CONST*M*M*4.0
      YN(4)=C12*A1+B1
      YN(3)=C12*A2+B2
      YN(2)=C12*A3+GA
      YN(1)=C12
      GN=GN/C12
      NNX=NN
      DO 10 I=1,NNX
   10 XN(I)=CN(I)
      NDX=ND
      DO 20 I=1,NDX
   20 YD(I)=YN(I)
      CALL PMPY(CN,NN,XN,NNX,YD,NDX)
   30 CONTINUE
      RETURN
      END
```

G LEVEL 21 BROWN DATE = 73110 22/12/09

```
      SUBROUTINE BROWN
C
C     BROWN'S HIGH FREQUENCY APPROXIMATION NO HEAT TRANSFER EFFECTS
C
      COMMON/GET/ANU,XL,CO,R,ZR,ZETA(200),TIME(200),JJ,WS,PO,NORDER,
     $SI,GA,TO,DT,TMAX
      RK=R*R/ANU
      PI=22.0/7.0
      AREA=PI*R*R
      ZO=CO/AREA
      TE=XL/CO
      A=1
      B=1
      D=-1
      TM=TMAX
      T=TO
      T1=TE*TE*A*A/RK
      T2=9*T1
      T3=25*T1
      T4=49*T1
      P1=D*D/RK
   80 DEL1=0
      IF (T.GE.TE) GO TO 10
      GO TO 20
   10 DEL1=1
   20 DEL2=0
      IF (T.GE.3*TE) GO TO 30
      GO TO 40
   30 DEL2=1
   40 DEL3=0
      IF (T.GE.5*TE) GO TO 50
      GO TO 60
   50 DEL3=1
   60 DEL4=0
      IF (T.GE.7*TE) GO TO 70
      GO TO 88
   70 DEL4=1
   88 SUM=0.0
      TERM1=0.0
      TERM2=0.0
      TERM3=0.0
      TERM4=0.0
      TERM5=0.0
      TERM6=0.0
      IF (T.LE.TE) GO TO 210
      ARG1=SQRT(T1)/(2.*SQRT(T-TE))
      TERM1=2.*EXP(-B*TE/RK)*DEL1*ERFC(ARG1)
      ARG3=P1*(T-TE)+SQRT(P1*T1)
      ARG4=SQRT(D*D*(T-TE)/RK)+SQRT(T1/(T-TE))/2.
      TERM3=2.*ZO*EXP(-B*TE/RK)*DEL1*EXP(ARG3)*ERFC(ARG4)/ZR
      IF (T.LE.3.*TE) GO TO 210
      ARG2=SQRT(T2)/(2.*SQRT(T-3.*TE))
      TERM2=2.*EXP(-3.*B*TE/RK)*DEL2*ERFC(ARG2)
      ARG5=P1*(T-3.*TE)+SQRT(P1*T2)
      ARG6=SQRT(D*D*(T-3.*TE)/RK)+SQRT(T2/(T-3.*TE))/2.
      TERM4=6.*EXP(-3.*B*TE/RK)*DEL2*ZO*EXP(ARG5)*ERFC(ARG6)/ZR
      IF (T.LE.5.*TE) GO TO 210
      ARG7=P1*(T-5.*TE)+SQRT(P1*T3)
```

G LEVEL 21 BROWN DATE = 73110 22/12/09

```
      ARG8=SQRT(D*D*(T-5.*TE)/RK)+SQRT(T2/(T-5.*TE))/2.
      TERM5=6.*EXP(-5.*B*TE/RK)*DEL3*ZO*EXP(ARG7)*ERFC(ARG8)/ZR
      IF (T.LE.7.*TE) GO TO 210
      ARG9=P1*(T-7.*TE)+SQRT(P1*T4)
      ARG10=
     $      SQRT(D*D*(T-7.*TE)/RK)+SQRT(T2/(T-7.*TE))/2.
      TERM6=2.*EXP(-7.*B*TE/RK)*DEL4*ZO*EXP(ARG9)*ERFC(ARG10)/ZR
  210 SUM=SUM+TERM1-TERM2-TERM3+TERM4-TERM5+TERM6
      SUM=SUM*PO
      JJ=JJ+1
      TIME(JJ)=T
      ZETA(JJ)=SUM
      WRITE(6,200) SUM,T
  200 FORMAT(20X,E15.8,20X,E15.8,/)
      IF(SUM.GE.PO) RETURN
      T=T+DT
      IF (T-TM) 80,80,90
   90 RETURN
      END
```

VITA

Balakrishna Mudunuri

Candidate for the Degree of

Master of Science

Thesis: DYNAMIC ANALYSIS OF A TRANSMISSION LINE TERMINATED BY A BISTABLE AMPLIFIER

Major Field: Mechanical Engineering

Biographical:

Personal Data: Born in Masulipatnam, India, January 25, 1947, the son of Annapurna Devi and Seshagiri Rao Mudunuri. Married Rajeswari on May 28, 1971.

Education: Graduated from Hindu College Higher Secondary School, Masulipatnam, India, in 1961; received the Bachelor of Science degree from Andhra University, Waltair, India, in 1964; received the Bachelor of Engineering degree in Mechanical Engineering from Andhra University, Waltair, India, in 1967; received the Master of Science in Engineering degree in Mechanical Engineering from Indian Institute of Science, Bangalore, India, in 1971; completed the requirements for the Master of Science degree at Oklahoma State University in May, 1973.

Professional Experience: Graduate Research Assistant in the Department of Mechanical Engineering, Indian Institute of Science, Bangalore, India, from August, 1967, to August, 1969; Teaching Assistant in the Department of Mechanical Engineering, Indian Institute of Science, Bangalore, India, from September, 1969, to August, 1971; Graduate Teaching Assistant in the School of Mechanical and Aerospace Engineering, Oklahoma State University, Stillwater, Oklahoma, from September, 1971, to December, 1972.